Sellia to Asomatos and the Cretan Detachment

View of the Kostifou Gorge looking North. The ridge in the background consists of Tripoliza limestone (Gavrovo nappe), which forms one of the upper nappes overlying the metamorphic Phyllite-Quartzite Unit.

Compiled by George Lindemann, MSc.

Berlin, August 2024

Contents

Appendix

1 Introduction

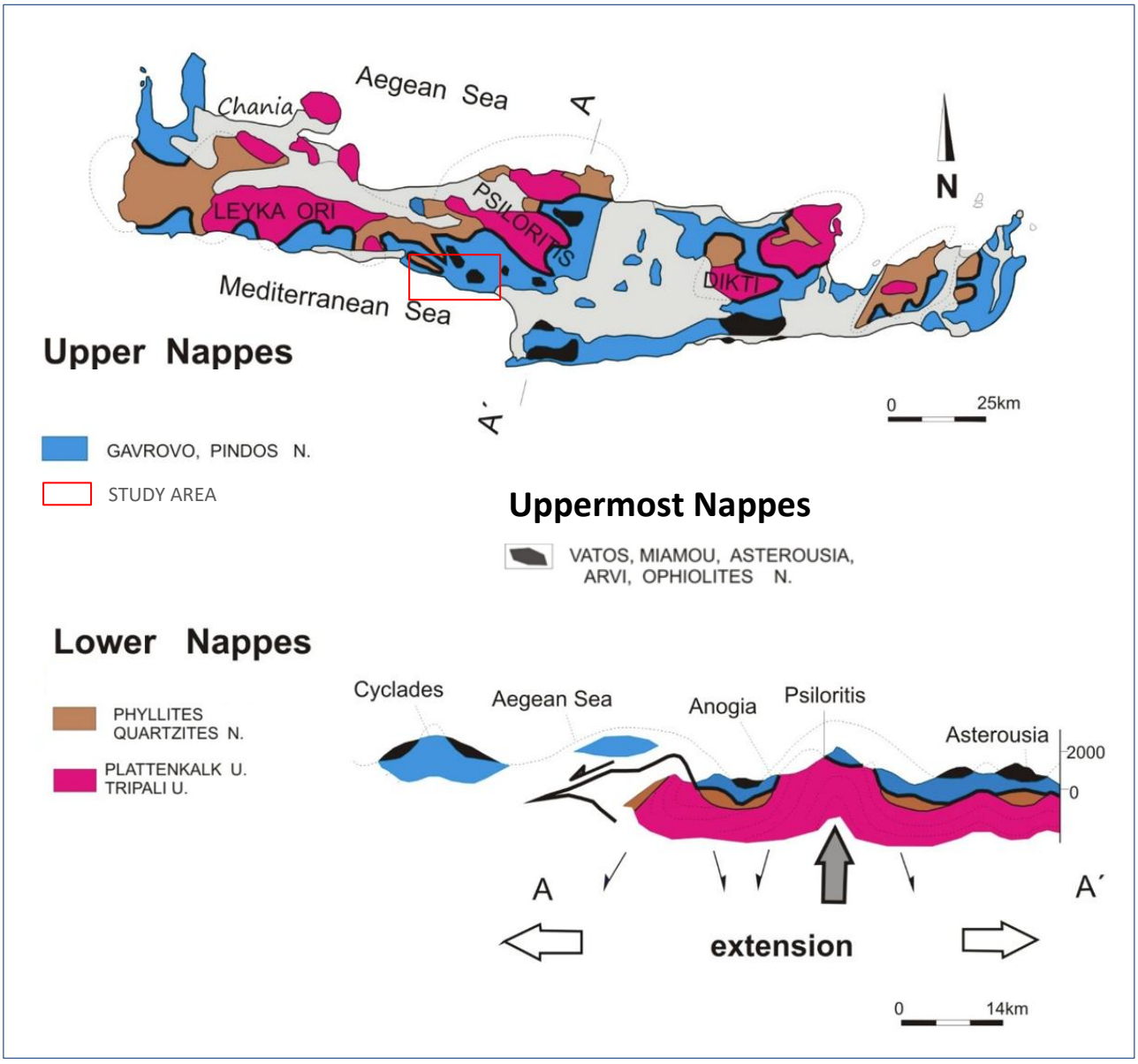

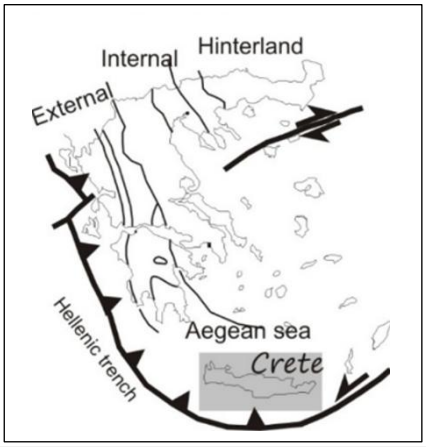

Source: Journal of the virtual explorer (NW Crete, online)

https://virtualexplorer.com.au/article/2011/285/neotectonic-study-of-western-crete/setting.html

The island of Crete is situated above the present-day Hellenic Subduction Zone of the eastern Mediterranean Sea and is one of the few places in the world where very young (Miocene) HP-LT metamorphic rocks are recognized as having been juxtaposed by extensional detachment (Fassoulas et al. 1994; Kilias et al. 1994; Jolivet et al. 1996) against nonmetamorphic rocks within a convergence zone dominated by oceanic subduction. From simple stratigraphic relationships, Crete has been shown to be composed of a series of thrust sheets or tectonic slices (Bonneau 1984), which were formed by collision of the northern margin of the Adria microcontinent with the southern margin of the Eurasian Plate during Oligocene and Miocene time at a convergent plate boundary dominated by subduction.

On Crete two main rock groups can be identified: a lower group comprising rocks that show pervasive Oligocene-Miocene HP-LT metamorphism, and an upper group that shows no evidence of Tertiary metamorphism. This major metamorphic break in the sequence has long been difficult to explain (see Robertson & Dixon 1984, p. 47). However, Lister et al. (1984) proposed a model where the HP-LT metamorphic rocks of Crete were exhumed along a shallow dipping extensional detachment from under a stretching and fracturing upper plate composed mainly of unmetamorphosed sedimentary rocks and ophiolite suite rocks. More recent studies by Fassoulas et al. (1994), Kilias et aL (1994), Jolivet et al. (1996) and Thomson et al. (1998a) also concluded, albeit with an opposite sense of motion along the extensional detachment, that the two rock groups must have been juxtaposed by a major low-angle extensional detachment sometime during the Miocene. It should be pointed out, however, that convincing exposures of a major detachment are difficult to find on Crete, as it is obliterated and cut by numerous Neogene cataclastic faults, landslips and slope screes. The proposals for major crustal extension on Crete rely mainly on the combination of indirect metamorphic, geochronological and structural criteria, as outlined by Wheeler & Butler (1994), to prove the occurrence of true crustal extension *[Thomson, 1998a]*. See also "No.16 My GeoGuide: Plakias Graben, Young faults and Neogene Continental Sediments; Appendix: Various Extensional Plate Tectonic Models".

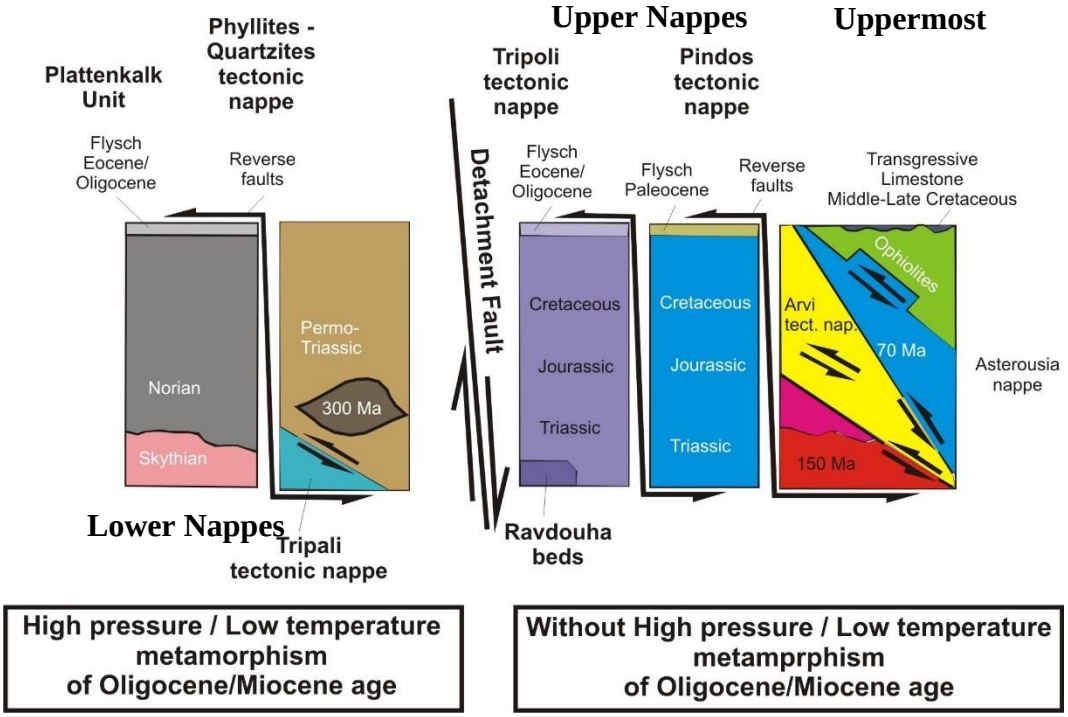

Tectonostratigraphic image showing the consecutive order of the various Cretan Nappes (slightly modified) [Source: Journal of the virtual explorer (NW Crete, online)].
https://virtualexplorer.com.au/article/2011/285/neotectonic-study-of-western-crete/setting.html

2 Sellia - Phyllite Quartzite Unit

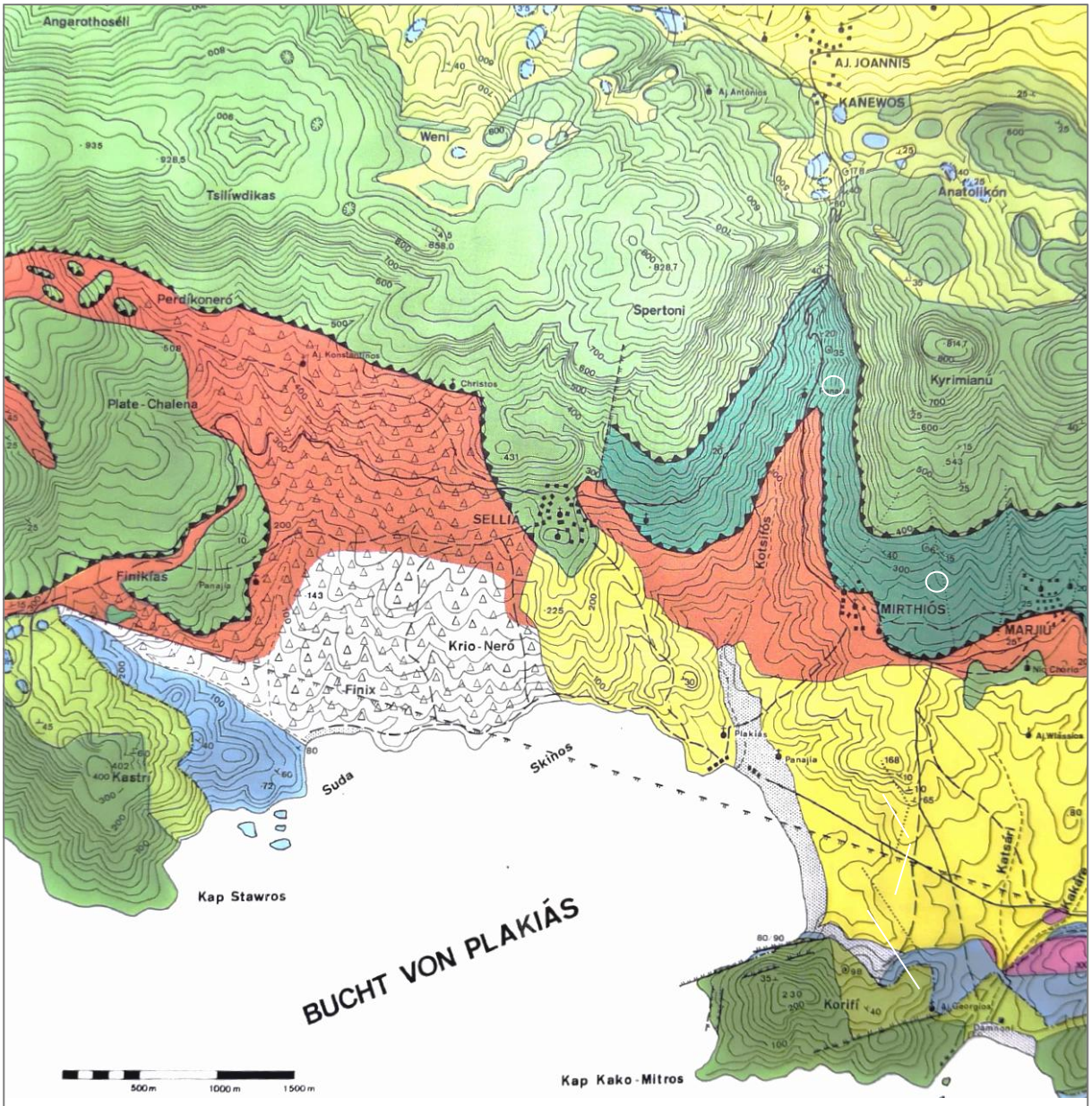

Geological Map of the area around Plaikas [modified after Miller W., 1977]

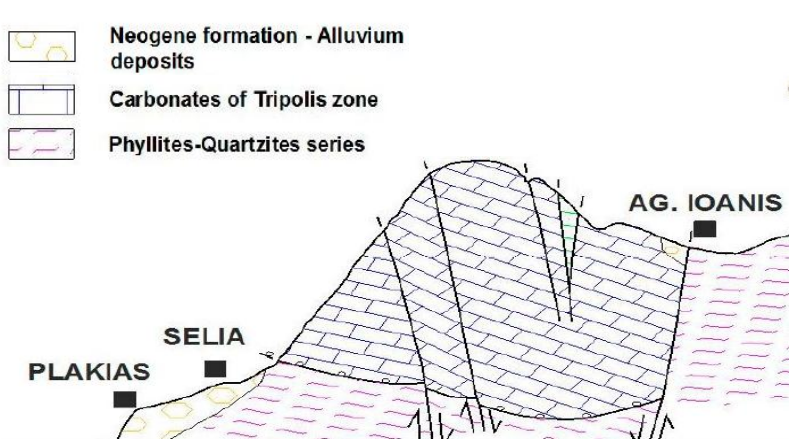

Hydrogeological section Plakias to Ag. Ioanis [Steiakakis E., 2017: Evaluation of Exploitable Groundwater Reserves in Karst Terrain]

2.1 Formation of the Phyllite-Quartzite Unit

The Phyllite-Quartzite Unit (PQ) on Crete is generally described as comprising of late Paleozoic to Triassic (Krahl et al., 1983) rock that was once deposited in marine siliciclastic, carbonaceous, and locally evaporitic sedimentary environments. The sedimentary rocks were deposited in shallow water on continental crust. The siliciclastic rocks occur mainly in the late Carboniferous to Permian stratigraphic units whereas the Triassic strata consist predominantly of carbonate rocks. The microcontinent carrying this sedimentary pile underwent a prolonged diagenetic history and eventually encountered the Hellenic subduction zone in mid-Tertiary times approximately 36 to 32 Ma ago (Thomson et al., 1998, 1999).

During the course of subduction, the stratigraphic units once overlying the mid-Triassic evaporites were detached and accreted at a shallow level; they are represented by the non-metamorphic rocks of the Tripolitza Unit (Bonneau. 1984; Thomson et al., 1999). In contrast, the PQ was carried down further by the subducted plate and was transformed by high pressure-low temperature (HP-LT) metamorphism. The siliciclastic rock consisting either of sandstone or shale was converted to quartzite and phyllite respectively, while the carbonate rock became marble. On its was way down the PQ became detached from its basement at a depth of about 35 km. Subsequently the PQ itself was underthrust by the more southerly part of the microcontinent, which was covered by the carbonate platform now forming the HP-LT metamorphic Plattenkalk Unit exposed beneath the PQ on Crete (B. Stockhert et al., 1998, Thomson et al., 1998, 1999).

Location of outcrops Ia and Ib west fo Sellia [source of image : Google Maps]

Outcrop Ia: Phyllite-Quartzite Unit (hammer for scale, arrow). 1: Phyllite, 2: Quartzite

Outcrop Ia: closeup showing phyllite and quartzite layers within the Phyllite-Quartzite Unit. 1: Phyllite, 2: Quartzite

Outcrop Ia: Sample of Phyllite displaying the shiny surface typical of phyllite caused by the growth of minute muscuvite and other sheet silicates at cleaverage planes (left: tip of hammer

head for scale). Phyllite represents the next progressive stage of metamorphism after shale and slate.

Outcrop Ia: Quartzite layer. Quartzite is a sandstone that has been transformed by metamorphism.

Outcrop Ia: closeup of a quartzite sample. Quartzite is characterized by its hardness as it contains mostly recrystallized quartz grains. The protolith (i.e. original rock) was most likely a sandstone. See My GeoGuide "No. 2 Mountain building western Crete north and south of Sfinari.pdf" for description of Quartzite and Phyllite

Outcrop Ib: Folds in silty phyllite and shear zone plane displaying cataclastic material. 1: Fold, 2: shear zone

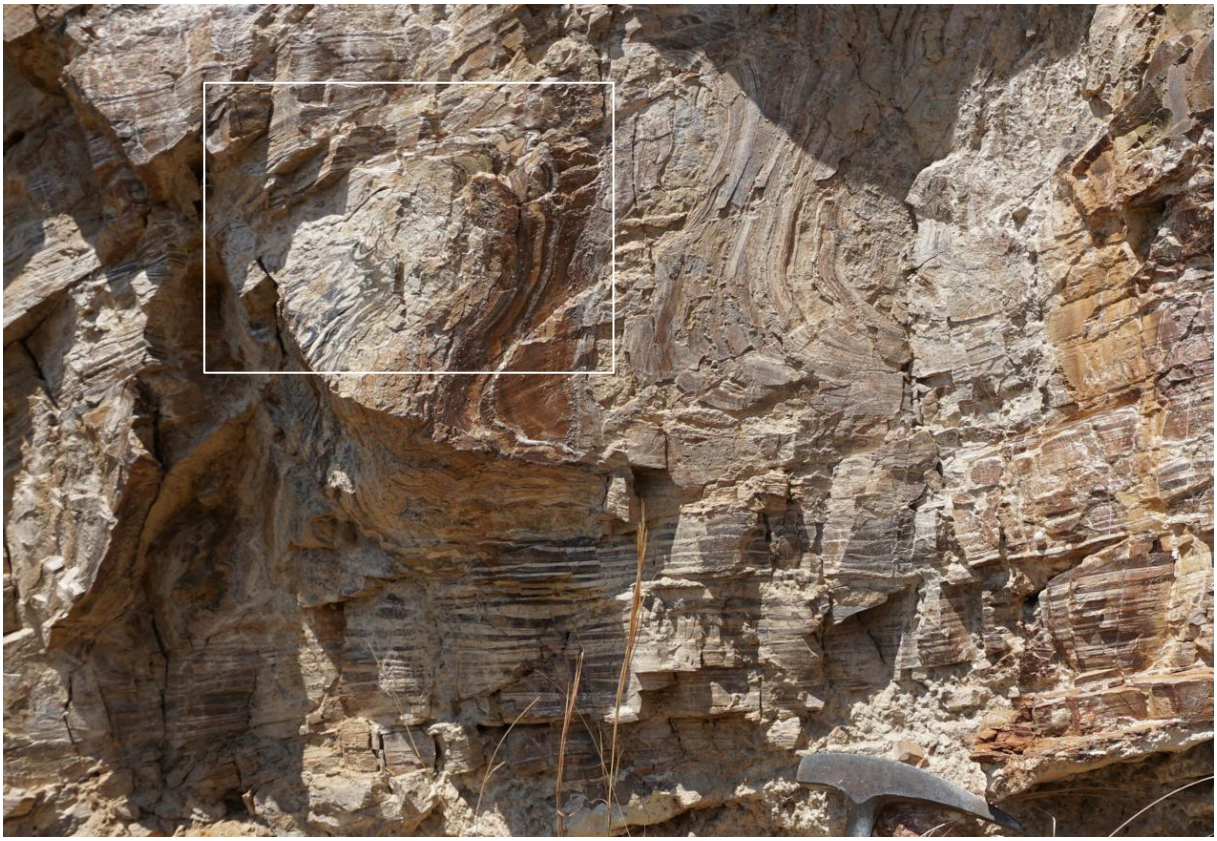

Outcrop Ib: Closeup of previous picture

Outcrop Ib: Closeup of previous picture showing parasitic M-folds. These are probably third generation folds due to their scale.

Outcrop Ib: Closeup showing details of fine phyllite and silicious silty layers. 1: Phyllite layer displaying cleavage, 2: Silicious silty layer possibly white chert.

2.2 Symmetry and Order of Folds

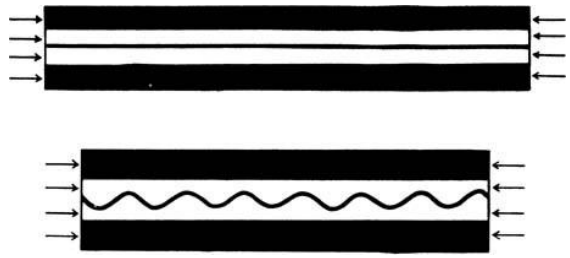

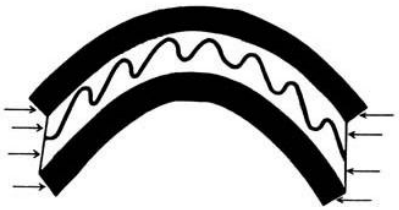

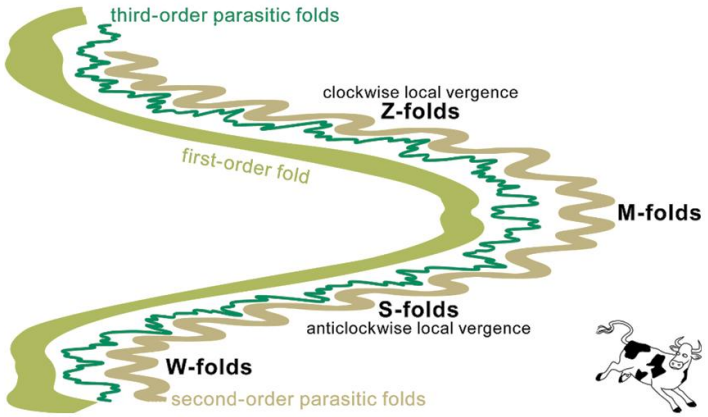

Source: jpd 2020

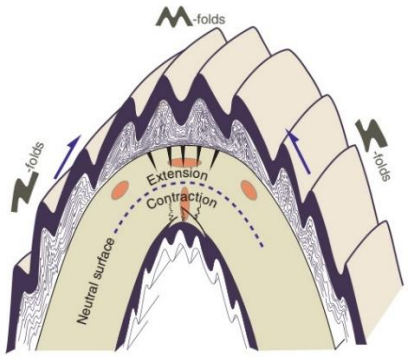

Source: Learning Geology , A Geology Outreach Website

http://geologylearn.blogspot.com/2015/08/geometric-description-of-folds.html

Symmetric folds are sometimes called M-folds, while asymmetric folds are referred to as S-folds and Z-folds.

Large folds tend to have smaller folds occurring in their limbs and hinge zones. The largest folds are called the first-order folds, while smaller associated folds are second and higher order folds. The latter are also called parasitic folds. First-order folds can be of any size, but where they are map scale, only second- or higher-order folds are likely to appear in outcrops. If a fold system represents parasitic (second order) folds on a first-order synformal or antiformal structure, then their asymmetry or vergence indicates their position on the large-scale structure. This relationship between parasitic and lower order folds can be useful for mapping out fold structures that are too large to be observed in individual outcrops. *(jpd 2020)*

View of Plakias beach and the Kotsifos Gorge. 1: Ravdoucha Beds, 2: Tripoliza limestone, 3: Phyallite-Quartzite Unit

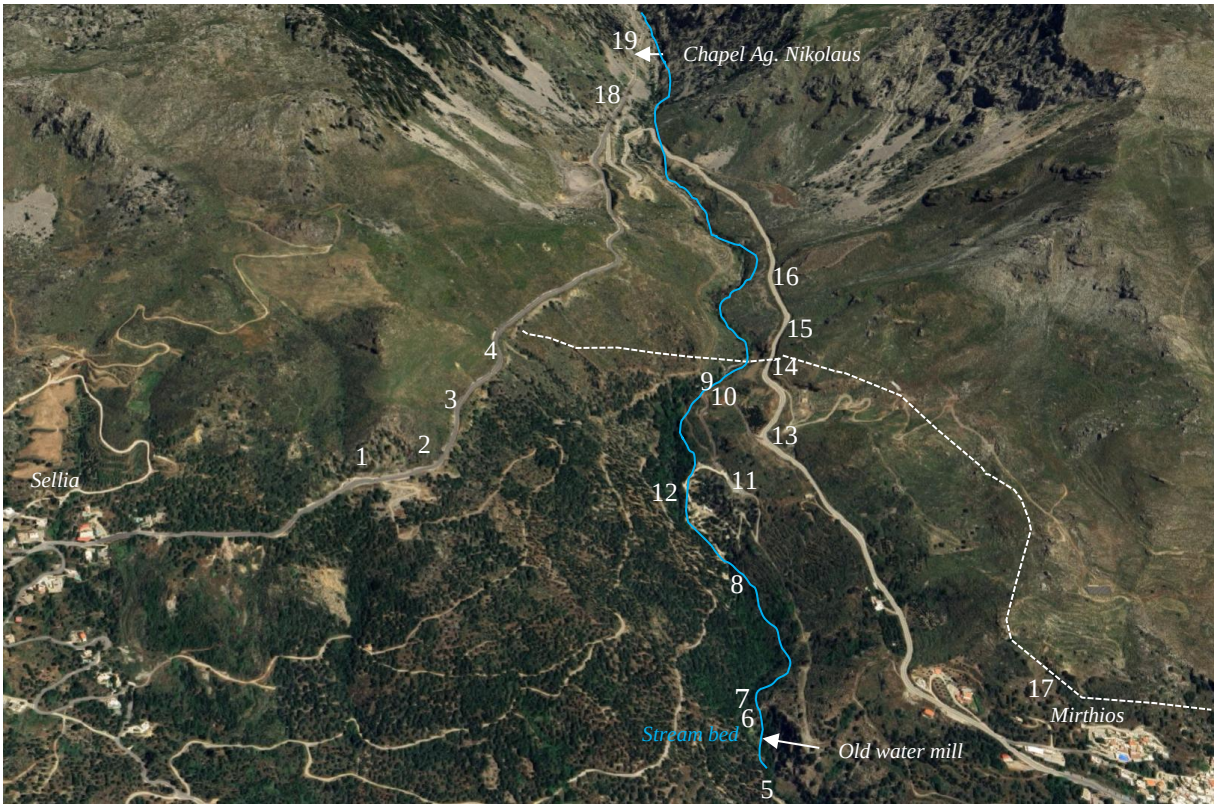

Overview of outcrops visited within the Kotsifou Gorge. Dashed line: presumed thrust plane between Tripolitza and Ravdoucha unit/ Phyllite-Quartzite unit [source of image : Google Maps]

3 The Western Side of the Gorge - Ravdoucha Beds and Transition to Tripoliza

From Sellia in an easterly direction, the Ravdoucha beds and the overlying Tripolitza limestone rocks are well exposed. Between the edge of the village and the entrance to the gorge the approx. 200m thick succession of Ravdoucha beds consists of dark dolomites and limestones, separated by dark and pink coloured shales and marl. The Ravdoucha beds are only weakly metamorphic and as such are tectono-stratigraphically positioned between the Phyllite-Quartzite Unit and the Tripolitza Unit. Originally, they are thought to have belonged the to the base of the Tripolitza unit. Being the more incompetent unit compared to the Tripoliza limestone, they were separated during the early stages of deformation, but at this location near Sellia (and Ravdoucha in NW Crete) the Ravdoucha Beds are thought to have retained their stratigraphic position. The Ravdoucha beds are indicated to corelate with the non-metamorphic part of the Tyros Bed in eastern Crete. *[Kull]*

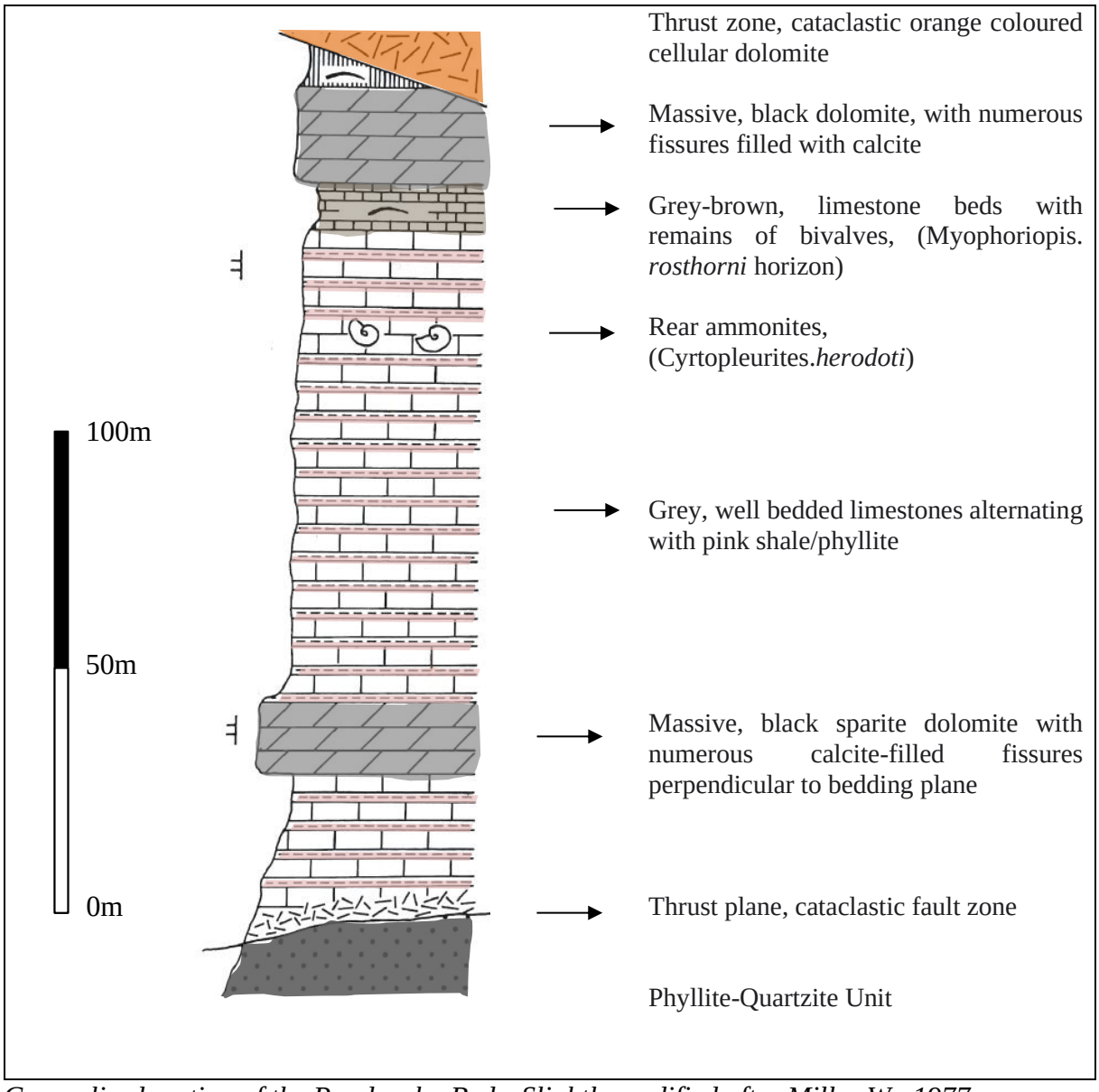

Generalized section of the Randovcha Beds. Slightly modified after Miller W., 1977

Location of Outcrops East of Sellia at the western side of the Kosifou Gorge

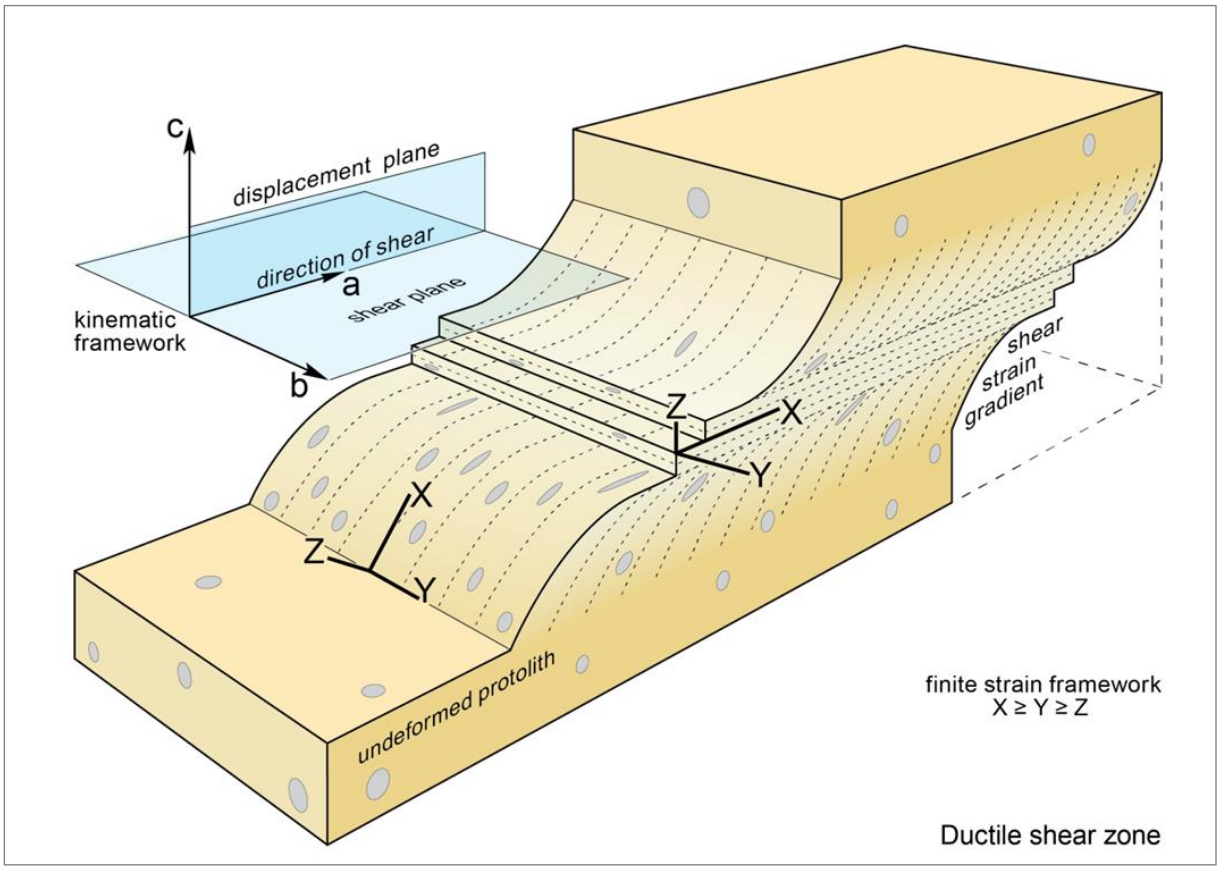

Diagram illustrating strain patterns within a ductile shear zone. Source: jpd 2020

Outcrop 1, Ravdoucha Beds. The Ravdoucha unit is only weakly metamorphic as opposed to the Phyllite-Quartzite Unit (PQ-Unit), which has undergone LT/HP metamorphism. The Ravdoucha unit tectono-stratigraphically occupies a position between the underlying PQ-Unit and the overlying Tripoliza Unit.

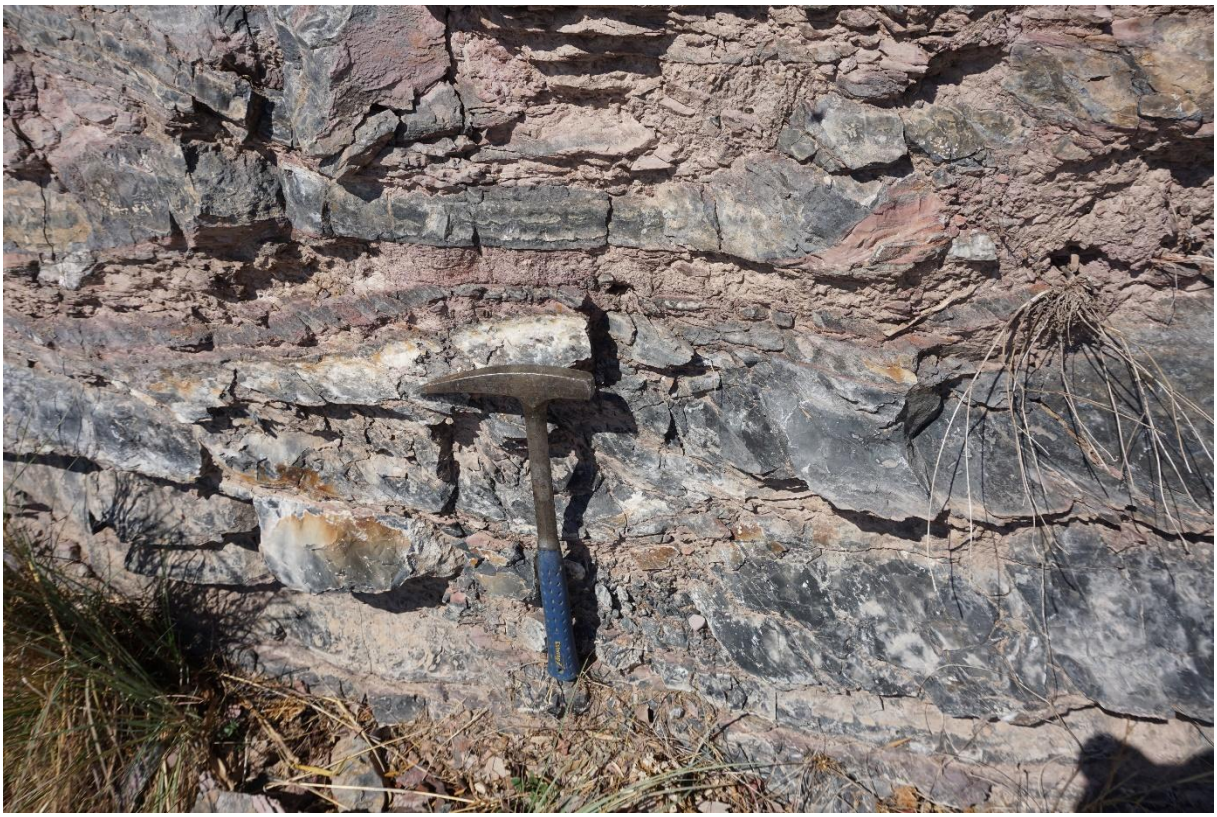

Outcrop 1, Ravdoucha Beds: Closeup showing a sequence of black organic-rich limestone and pink shale.

Outcrop 1, Ravdoucha Beds. Disharmonic detachment fold. Detachment folds often appear in less competent rock such as shale sandwiched between harder rocks. Under stress the incompetent layers may detach from their more stable underlying layer.

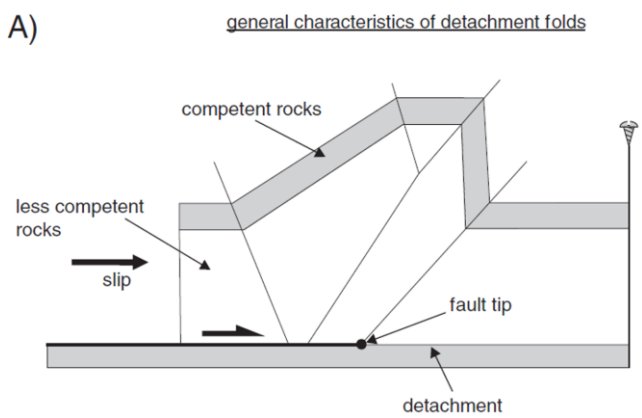

A) General characteristics of detachment folds are a horizontal detachment and a core of less-competent rocks.

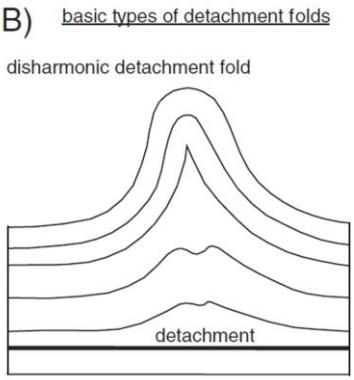

B) Types of detachment folds: 1. fold coreis characterized by disharmonic folds [Brandes C. et al., 2014]

Outcrop 2, Ravdoucha Beds. Stack of isoclinal folds (left), fault on the right

Outcrop 2, Ravdoucha Beds. Closeup of the right side of the previous picture

Outcrop 3. Bedding and sequence of pink shale and dark limestone belonging to the Ravdoucha beds.

Outcrop 3, Ravdoucha Beds: shear zone. 1: incompetent thin sequence of shale and carbonate beds, 2: Thick competent limestone with numerous calcite veins resulting from fracturing and secondary crystallization of calcite.

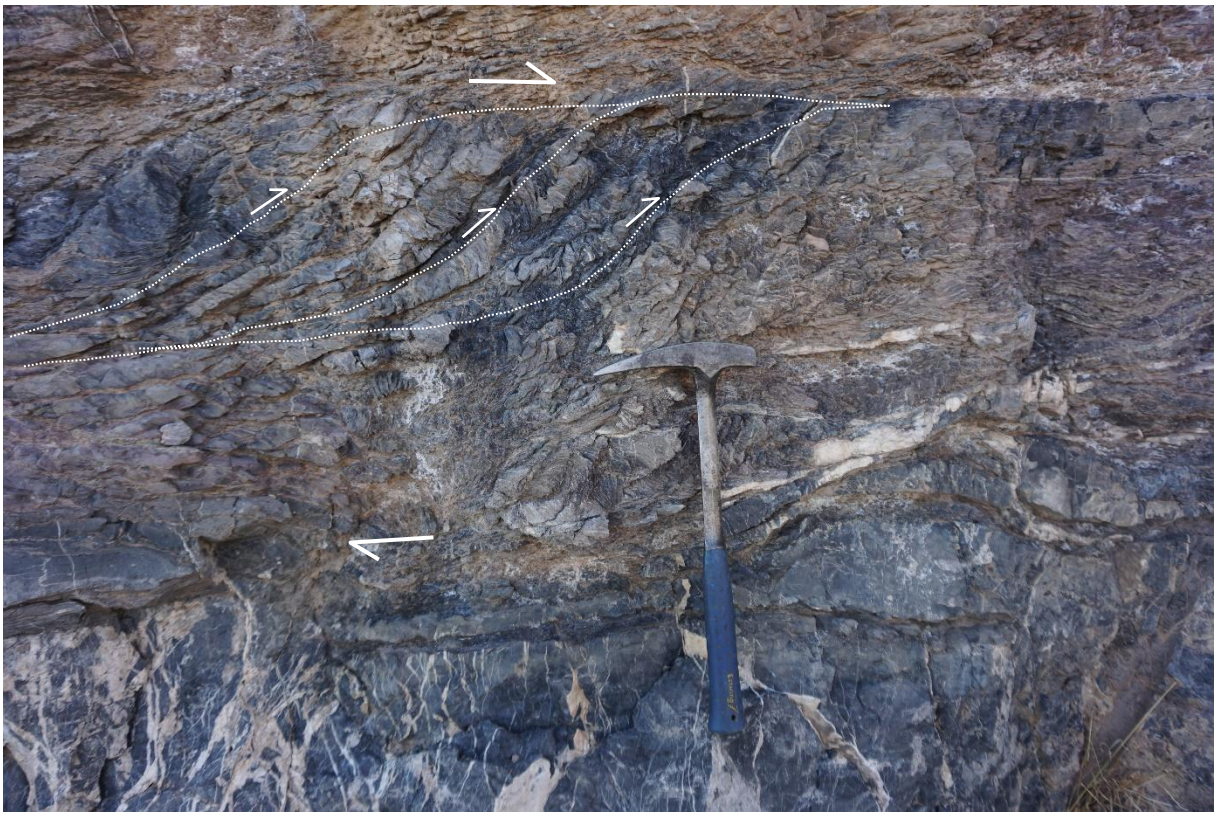

Outcrop 3, Ravdoucha Beds. Duplex link thrusts. Link thrusts: imbricate thrusts that link the floor thrust to the roof thrust of the duplex. Link thrusts are commonly sigmoidal in shape (McClay & Insley)

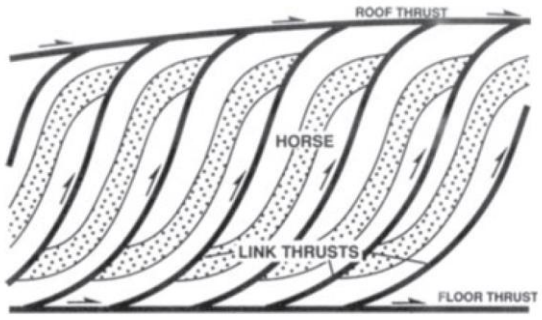	*Link thrusts and duplex structures [McClay K.R.: Glossary of thrust tectonics terms]*

Outcrop 3, Ravdoucha Beds. Calcite veins in black limestone similar to those observed in the Kotsifou river bed.

Outcrop 3, Ravdoucha Beds. Highly sheared incompetent pink shale beds (1) and highly jointed/fractured limestone beds (2).

3.1 Drag folds in Shear Zones

The term *drag fold* refers to a certain kind of fold with quasi monoclinic symmetry that usually, but not exclusively, occurs on the limbs of larger folds. The relatively thin layers that show drag folding are usually embedded in incompetent (soft, weak, or compliant) rocks that in turn are sandwiched between thick competent beds.

The vergence of asymmetric fold trains in shear zones is generally unrelated to lower-order folds and can give information about the sense of shear of the zone. Such kinematic analysis requires that the section of observation contains the shear vector and should be used together with independent kinematic indicators. *Credits: Haakon Fossen (Structural Geology)*

Outcrop 3, Ravdoucha Beds: drag folds within a shear zone

Outcrop 3, Ravdoucha Beds: Closeup of previous picture

Outcrop 3: Closeup of previous picture

4 Transition to Tripoliza Limestone - Cellular dolomite

Outrop 4. Cellular dolomite/Rauhwacke. At this location the cellular dolomite, being a highly incompetent layer, is thought to represent an intensive shear zone between the Tripoliza limestone and the Ravdoucha unit.

Outrop 4: Closeup of previous picture.

Outcrop 4: Closeup of previous picture

5 The Stream Bed – Phyllite Quartzite Unit and Ravdoucha Beds

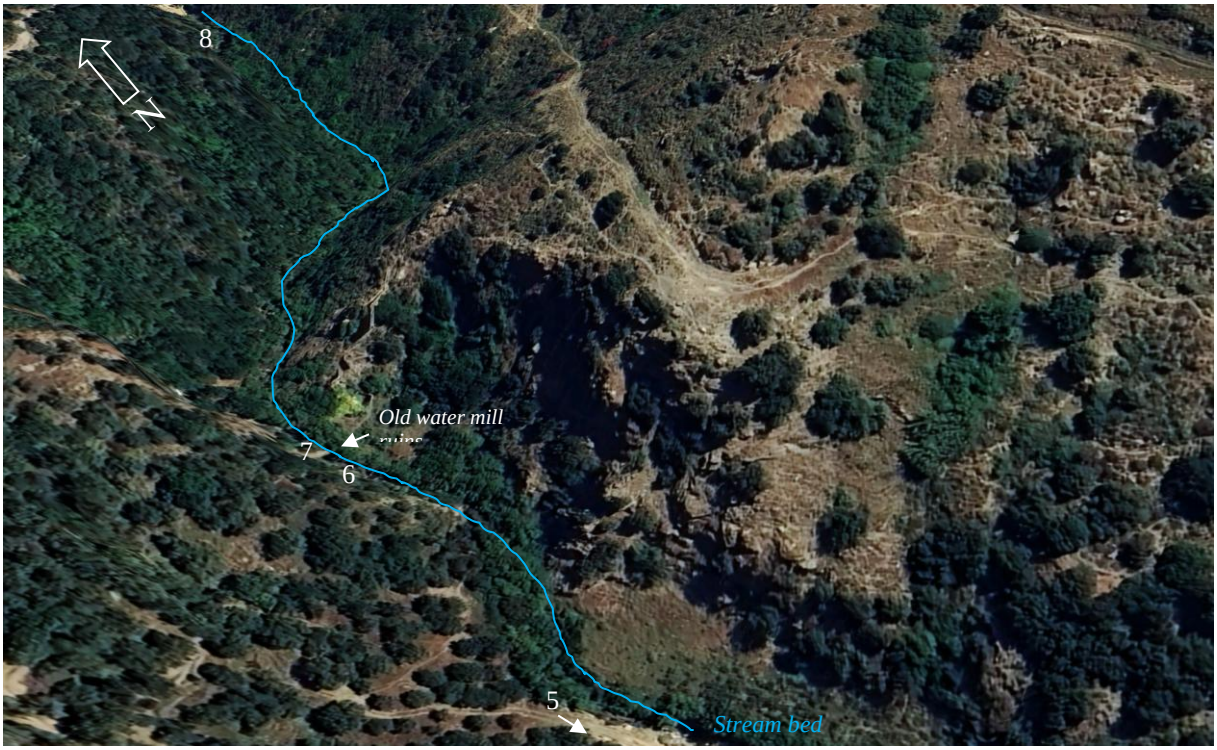

Location of outcrops [source of image Google Maps]

View of the entrance to the Kotsifou Gorge and the outcropping rocks.

Outcrop 5, Phyllite-Quartzite Unit: Phyllite displaying typical shiny surface of foliation planes.

Outcrop 5: Close up of privious picture

Outcrop 6: Phyllite-Quartzite Unit: phyllite wrapped (anastomosed) around quartzite lenses. Ductile shear zones frequently show anastomosing geometries of highly-strained rocks around lozenges of less deformed material (hammer for scale see arrow).

Outcrop 7: Phyllite-Quartzite Unit. Phyllite displaying joints at right-angles to foliation.

View of the aqueduct leading to the top of the mill, where water was once directed onto the water wheel. At the opposite side of the gorge the Phyllite-Quartzite layers dip northwards and appear to be part of a limb of a large fold.

Outcrop 8: Phyllite-Quartzite Unit exposed in the stream bed of the gorge. Greenschist indicates the existence of former volcanic or igneous rock.

Outcrop 9: Limestone located in the Kotsifou stream bed. Possibly Ravdoucha beds, owing to the similarity of the beds at Outcrop 3. The dark limestone displays numerous secondary calcite veins indicating brittle deformation occurring either during or after folding. 1: bedding plane, 2: Orientation of veins is at right angles to bedding.

Outcrop 9: Closeup of previous picture. The dark colour is due to high organic content.

Outcrop 10: Tectonic breccia within the Tripolitza limestone represents the fault zone between the Tripolitza nappe and the Ravdoucha Unit.

6 Eastern side of the Kotsifou Gorge - Phyllite Quartzite Unit and Ravdoucha Beds

Location of Outcrops. Lines indicate off-set of major north-south trending fault [source of image Google Maps]

Outcrop 11. This location at the eastern side of the gorge about 30m below the main road, displays the Phyllite-Quartzite Unit with lens-shaped structures. The lens- or lozenge-shaped structures are the result of shear stresses. The lenses or are not sigmoida-shaped indicating that no rotation has taken place along this section (i.e., exposed plane) of the outcrop.

Outcrop 11: A fault has off-set the black phyllite layer by about half a meter. In some places the phyllite appears to have been wrapped around the more competent quartzite lenses.

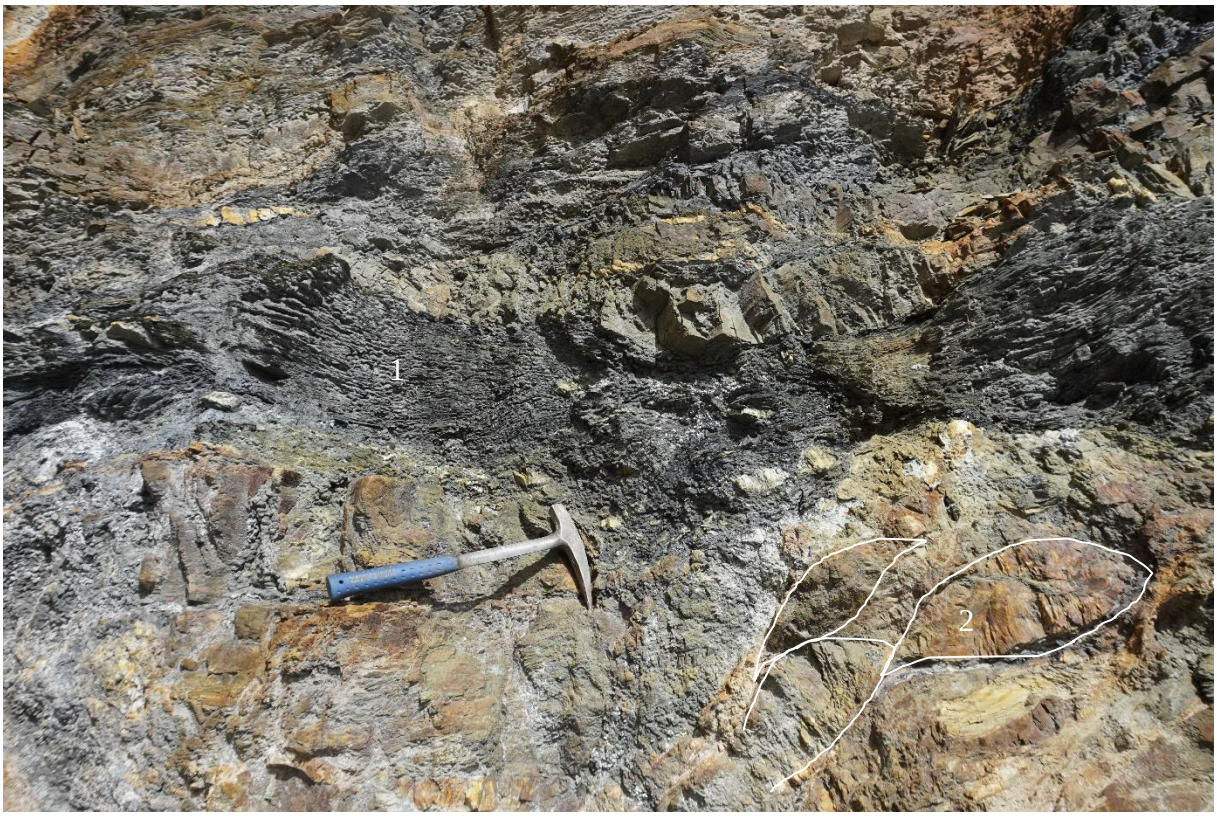

Outcrop 11. 1: Black organic phyllite layer, 2: Quartzite partly stained brown-orange probably by iron-rich water from small spring. The lens shapes are the result of shear stress.

6.1 Lozenge-Shaped Patterns

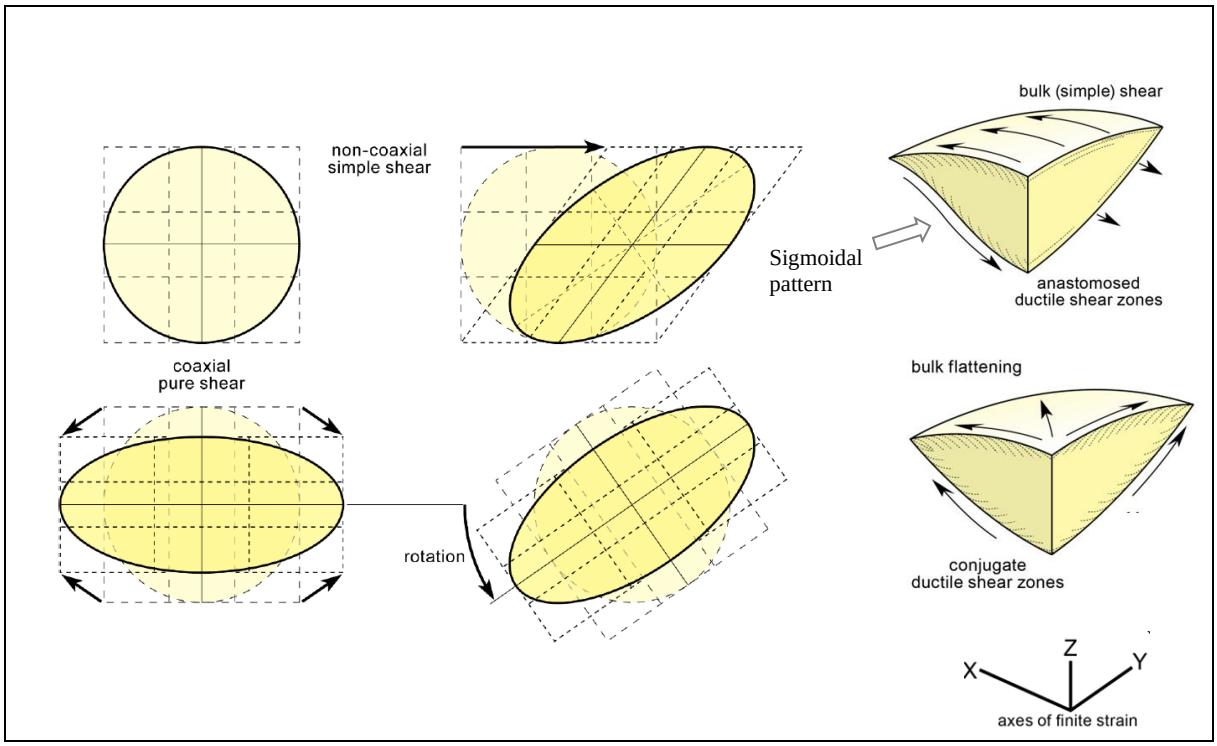

Relationship between shear zone pattern, kinematics and bulk finite strain. Source: (Finite strain, jpd 2020).

Shear zones often anastomose around lenses of less deforme[illegible]ıtry rock. The shape of the rock lenses may be divided into three types depending on the regional deformation regime:

- Rod-shaped or cigar-shaped lenses indicate constriction (see Appendix).
- Lozenge-shaped lenses indicate near plane strain.
- Flattened rock lenses indicate the flattening field of bulk finite strain.

Conjugate shear zones indicate bulk coaxial deformation; shear zones with identical sense of shear denote bulk non-coaxial deformation.

Outcrop 12: Directly across the gorge, the western valley wall consists of folded Tripoliza limestone indicating a major normal fault that has off-set the PQ-Unit and Tripoliza unit. In this case the Tripoliza unit being the younger formation must have been down thrown and therefore belong to the hanging wall.

6.2 Phyllite Quartzite Unit

Outcrop 13: Phyllite-Quartzite Unit exposed at the main road at the eastern side of the gorge.

Outcrop 13: the Phyllite-Quartzite Unit at this location displays abundant phyllite rock.

Outcrop 13: Phyllite-Quartzite Unit. Phyllite sample displaying shiny surface and light green colour. The shine is due to microscopically small sheet silicates such as muscovite and sericite formed during metamorphism. The green colouring can be attributed to minerals such as chlorite. The Phyllite-Quartzite Unit is reported to have undergone low temperature / high pressure (LT/HP) metamorphism that is common in subduction zones.

Outcrop 13. View of the eastern side of the gorge looking north. There is a major fault zone between the Phyllite-Quartzite Unit and the Tripoliza Nappe. At this location the base of the

Tripoliza unit is composed of cell dolomite. Apparently the Ravdoucha Beds have been off-set so that they are no longer visible within the fault zone.

6.3 Cellular Dolomite

Outcrop 14. Cataclastic cell dolomite at the major fault zone between the Phyllite-Quartzite Unit and the Tripoliza Nappe displaying a chaotic, coarse-pored, brown to ochre-yellow texture (rucksack at bottom centre of picture for scale).

Outcrop 14. Brecciated cell dolomite

Outcrop 14: Brecciated cell dolomite, closeup of the previous picture. The cavities are reported to have been created by the solution gypsum. This would infer that the rock was originally deposited in a shallow coastal environment to enable the formation of evaporites. During a later phase, tectonic processes must have crushed the rock forming the breccia structure.

Outcrop 14: Brecciated cell dolomite

Outcrop 14: Brecciated cell dolomite. In this sample the cavities contain a yellowy powdery substance, which is probably a type of Fe-oxide.

Outcrop 14: Brecciated cell dolomite displaying several phases of brittle deformation. 1: dark clasts (containing even smaller clasts) indicate a second phase of brecciation 2: The light matrix also contains small clasts. Thrusting of the Tripoliza Nappe for example within accretionary wedge of a subduction zone will have caused high friction and crushing along the thrust plane.

Outcrop 14: Cell dolomite displaying secondary crystals thought to be either dolomite or barite.

6.3.1 Origin of Cellular Dolomite / Rauhwacke

Rauhwacke is also known as cellular dolomite. The rock consists of dolomite with cavities formed by the leaching of water-soluble gypsum. The gypsum embedded in the dolomite was formed early in the rock's genesis. The process encompassed the precipitation of evaporites and the early-diagenetic dolomitization of lime muds. During nappe tectonics and extensive thrusting, the gypsum layers served as a type of lubricant upon which the nappes could travel. This is because evaporites form incompetent layers that are easily deformed. Along the thrust planes the rocks were faulted and brecciated forming a polymict mixture of dolomite and gypsum clasts. Dissolution of the gypsum clasts is thought to have been the result of fairly late karst processes, when leaching of evaporite minerals lead to the collapse of the overlying sediments (Beales and Hardy, 1980; Friedman, 1997). What remains are the cavities or cells that gives Rauhwacke its name. The absence of any folding, schistosity and open fracture structures indicates that the mechanical properties of the Rauhwacke differ fundamentally from those of the surrounding Tripoliza and Phyllite-Quartzite rocks (https://nationalpark.ch/flora-und-fauna/rauhwacke/)

The term polymict refers to the composition of clastic sedimentary rocks that are made up of different types of components. The opposite of polymict is monomict

Outcrop 15: Folded and faulted Tripoliza limestone (rucksack at the edge of the road for scale)

Outcrop 15: Folded and faulted Tripoliza limestone

Outcrop 16: a small exposure of the Ravdoucha Beds

Outcrop 16. Ravdoucha formation displaying alternating pink shale beds between finely laminated dark limestone beds.

7 Mirthios, Phyllite-Quartz Unit and Tectonic Breccia

Outcrop 17. This location lies near Mirthios within the fault zone between Phyllite-Quartzite Unit and the Tripoliza unit [source of image Google Maps]

Outcrop 17, Phyllite-Quartzite Unit

Outcrop 17, closeup of previous picture showing a sample of quartzite containing metamorphic minerals. 1: possibly sillimanite, 2: dark rhombic-shaped mineral, possibly titanite.

Outcrop 17: Lithified tectonic breccia (Tripoliza) exposed a few meters above the quartzite (Phyllite-Quartzite Unit)

Outcrop 17: Closeup of previous picture displaying different sized clasts of varying composition. The smaller clasts in the matrix are more angular (possibly quartz) whereas the larger clasts are more rounded and consist of limestone.

Outcrop 17: A closeup of the tectonic breccia. The rock is quite hard and has supposedly undergone metamorphism. The texture displays numerous cavities and is presumably the same rock as the brecciated cellular dolomite found within the Kosifou Gorge. The cataclastic texture indicates the presents of a shear zone between the Phyllite-Quartzite Unit and the Tripoliza limestone.

8 The Tripolitza Unit

The Tripolitza limestones and dolomites that overlie the Ravdoucha Beds of central Crete may be generally described as having a thickness of approx. 1000 m. The carbonates were deposited in a shallow marine environment on a long-term stable platform. The carbonates that range from the Lower Triassic to the Eocene are partly well bedded and display predominantly micritic to micro-sparitic textures under the microscope. The predominantly grey carbonates occasionally display dark organic rich beds. Macro fossils are spars, but abundant microfossils indicate that there were no long-term breaks in sedimentation. Lagoonal algal limestones with dasycladaceans occurred in the Middle and Upper Jurassic (see Appendix) *[Kull]*.

A study of a small sequence of the Tripoliza carbonates within the Kotsifou Gorge indicates the presents of peritidal lagoonal conditions during the Lower Jurassic. The dolomites display cyclic sedimentation and are interbedded or capped by laminar calcretes, which is evidence of prolonged subaerial exposure and soil forming conditions. Laminated dolomites evolved during the Lower Cretaceous and rudist biostromes existed in the Upper Cretaceous. Alveolin-algal bioherms and nummulite limestones were formed in the Paleogene *[Pomoni, 2016]*.

Work in the Dikte Mountains by Zambetakis-Lekkas et al., 1995 reveals similar conditions for the Upper Cretaceous based on the presents of stromatolite limestones. During the course of the Upper Cretaceous, after a temporary deeper shallow marine event in which rudist reefs existed, increasingly shallow marine lagoonal conditions led to frequent subaerial exposure in the Maastrichtian and interruption of sedimentation in the Paleocene *[Kull]*.

Flysch sedimentation resulting from the emerging orogen took place in the Eocene (Wachendorf et al. 1980). The flysch consists of a sequence of shales, marls, sandstones, graded limestone breccias and conglomerates with rock components of the Eurasian plate (Hall et al. 1984) and ophiolite detritus. The thickness of the flysch is approx. 200 m or more. The youngest parts of the flysch are probably of Lower Oligocene age.

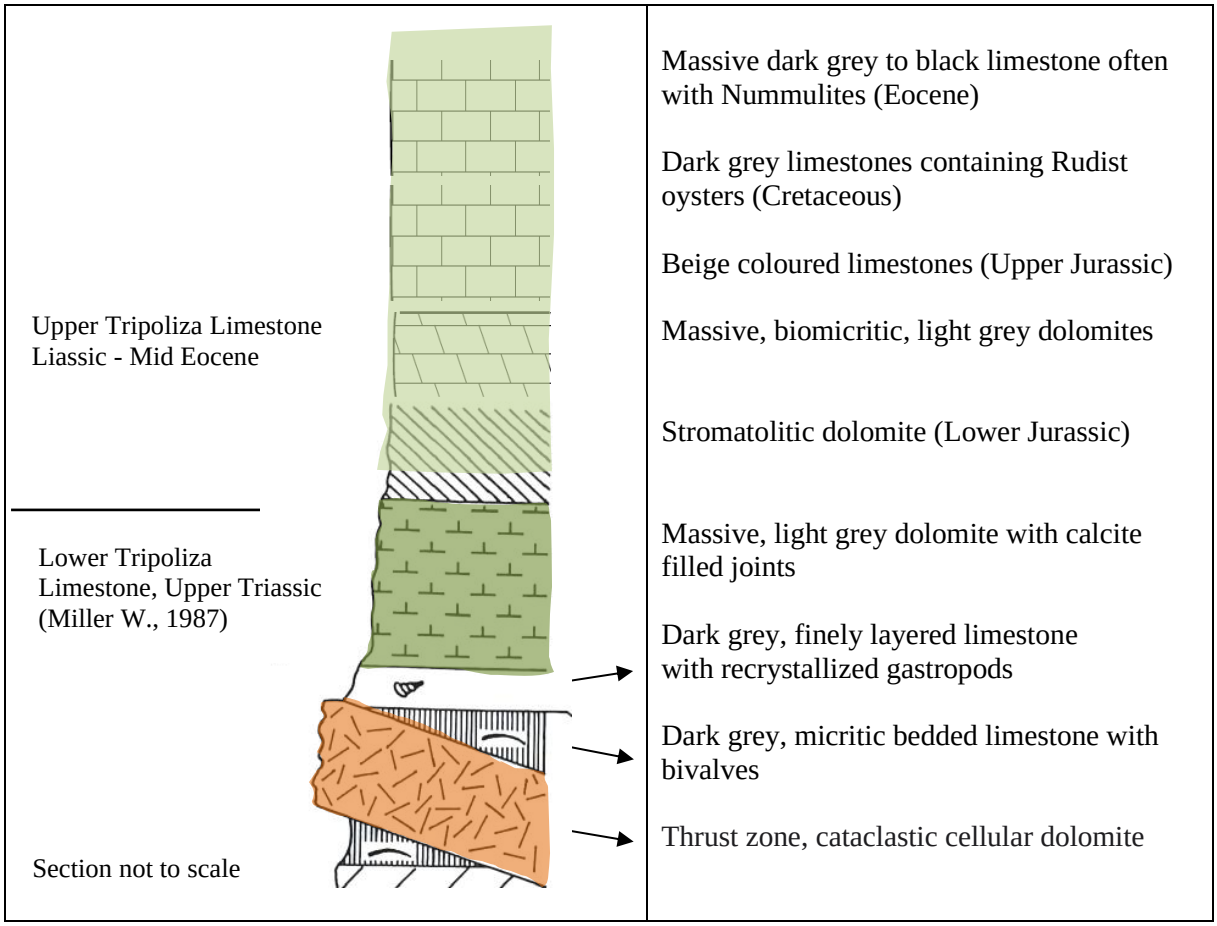

Generalized section of the Lower and Upper Tripoliza Limestone (based on W. Miller, 1987)

Outcrop 18: Well bedded Tripolitza limestone (probably Lower Tripoliza Limestone)

8.1 Upper Tripolitza Limestone

The total thickness of the Upper Tripoliza Limestone is estimated at 900 m. The contact with the underlying Lower Tripolitza Limestone is sedimentary and is thought to begin with the stromatolitic dolomites, which are light to dark grey in colour (Müller, 1987). The stromatolitic dolomites occur frequently in the area between Sellia and Asomatos in the same stratigraphic position and therefore represent a good marker horizon. The approximate age of the stromatolitic dolomites is indicated to be Lower to Middle Liassic age (Pomoni F. 2016).

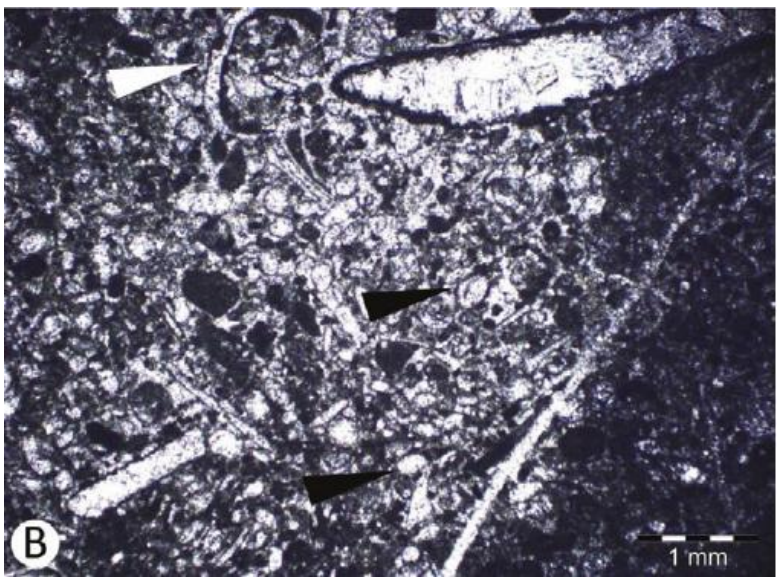

Examples from the stromatolitic dolomite beds representing a shallow subtidal to intertidal fenestral facies (microscopic image under polarized light).

B: Dolomitic packstone to grainstone with ostracods (black arrows) and sparse bivalves (cortoids, white arrow).

Note a large cortoid on the upper right corner of the section

	(Source: Pomoni F. 2016)
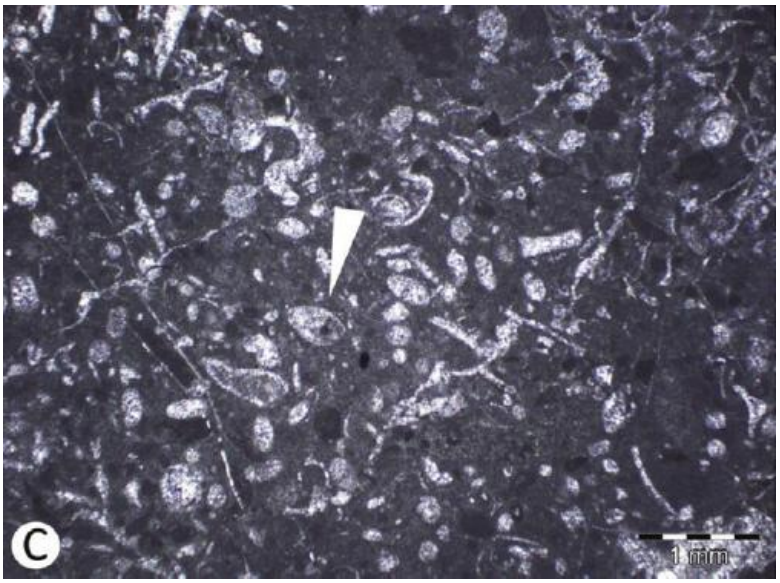	*C: Dolomitic floatstone with ostracods (arrow), bivalves, gastropods and occasional benthic foraminifera (Source: Pomoni F. 2016)*

The stromatolitic dolomites form well bedded cyclotherms of dm- to cm-thickness and are frequently capped by dolomitized laminar calcretes. Each cycle starts with relatively open marine facies, which are overlain by shallower, more restricted facies (tidal flat progradation). Within the stromatolitic dolomites two lithofacies associations have been recognized by Pomoni F., 2016 - one corresponding to a shallow subtidal to intertidal environment with bioclasts, intraclasts and peloids, implying a moderately high-energy level and deposition in an inner-ramp carbonate setting (tidal flat) and one consisting of laminar dolocretes, which are calcified root-mats forming irregular, contorted micrite laminae during episodes of subaerial exposure.

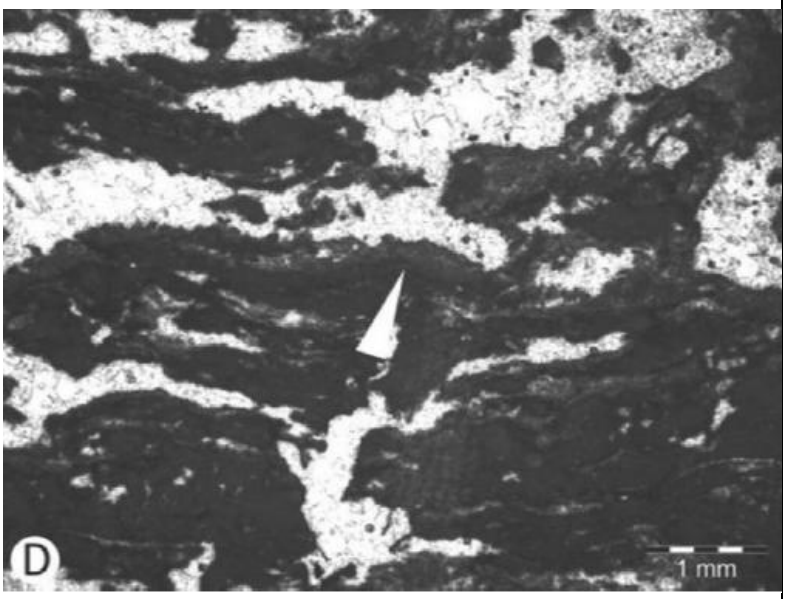	*Example of a laminar dolocrete under the microscope* *D: calcified root mats (black to dark gray). Note internal sediment introduced between the laminae (lighter gray, arrow) and parallel and perpendicular to bedding irregular fenestrae cemented by "flower-spar" dolomite. Macroscopically the root mats may resemble algal microbial stromatolites, but they do not thicken upwards, as do the domed laminations typical of stromatolites (Bernoulli and Wagner, 1971; Waite et al., 2013). (Source: Pomoni F. 2016)*

The formation of cyclothems is reported to reflect a combination of Milankovitch-related eustasy and uniform tectonic subsidence (allocyclic processes), in a ramp-to-shelf carbonate system with tidal flat and restricted lagoon environment. Sea-level changes and subsidence rates were the decisive factors influencing sedimentation.

Outcrop 18. Upper Tripolitza Limestone. Layers stromatolitic dolomites/ root mats

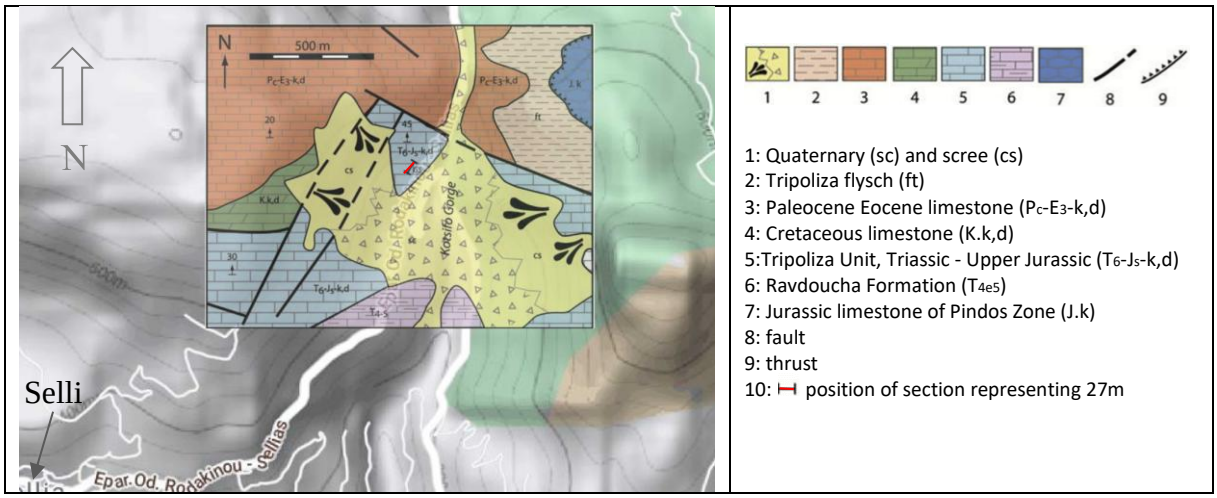

Geological map of the Kotsifou Gorge area. [Pomoni F. 2016]

South of Mount Kyrimianu, within the Kotsifou gorge the stromatolitic dolomites are initially overlain by massive, fine-grained, light grey dolomites, which gradually change into beige coloured limestones. Some of these are coarse-grained and have a thickness of 300m. Macro fossils are rare in the beige coloured limestones. However, its stratigraphic position between the stromatolitic dolomites and overlying Cretaceous rudist limestones indicates Upper Jurassic age.

Outcrop 19: The chapel Ag. Nikolaus is located northwards further up the gorge and is built into the Upper Tripolitza Limestone. The grey limestone and dolomite is more massive at this location and it is reported to contain nummulite foraminifers.

8.2 Formation of Dolomite

Dolomitization is the process in which primary calcite or aragonite is replaced by secondary dolomite. On the one hand, dolomitization can take place by replacing Ca ions with Mg ions with simultaneous supply of Mg^{2+} and removal of Ca^{2+}, according to the reaction

$$Mg^{2+} + 2(CaCO_3) \rightarrow CaMg(CO_3)_2 + Ca^{2+}.$$

On the other hand, Mg^{2+} and CO_3^{2-} can also be supplied by dolomitizing fluids alone according to the reaction

$$CaCO_3 + Mg^{2+} + CO_3^{2-} \rightarrow CaMg(CO_3)_2$$

Dolomitization can be syn-sedimentary/early diagenetic and late diagenetic. All models of dolomitization have in common that fluids with a very high Mg-Ca ratio of 5-10 are held responsible for dolomitization. According to the Sabkha model, such waters are formed by intensive evaporation of seawater in salt pans with simultaneous precipitation of calcium carbonate. However, the majority of dolomite rocks are thought not to be associated with supratidal environments. For these, the mixing model is based on the dilution of seawater by fresh groundwater to initiate dolomite formation. Hereby the Mg-Ca ratio is maintained while salinity decreases (see Appendix).

9 Mariou

9.1 Phyllite Quartzite Unit

Location of Outcrops [source of image: Google Maps]

Outcrop I: Phyllite-Quartzite Unit underlying Tripoliza limestone nappe (overlying nappe not visible in this photo)

Outcrop I, Phyllite-Quartzite Unit: Phyllite displaying characteristic shiny surfaces and good foliation.

9.2 Segment of Folded Tripoliza Limestone

Outcrop II. Fault zone between Tripoliza limestone and weathered schist. Further to the right porous carbonate presumably Neogene or Quaternary sinter deposits. 1: Fold in Tripoliza limestone, 2: Fault zone, 3: Highly weathered calcsilicate schist (Phyllite-Quartzite Unit) 4: presumably cellular dolomite.

Outcrop II. Anticline and syncline within Tripoliza limestone near the detachment fault (hammer for scale, arrow)

Outcrop II, fault zone. 2a: Breccia with Tripoliza limestone clasts, 2b: mixed clasts, 2c: highly weathered calcsilicate schist

Outcrop II, fault zone. Closeup of previous picture. 2c: highly weathered calcsilicate schist

Outcrop II, highly deformed and weathered calc-silicate schist

9.3 Ravdoucha Beds

Outcrop III, presumably Ravdoucha beds owing to thin pink shale layers between black limestone beds.

Outcrop III, presumably Ravdoucha beds. 1: black thinly bedded limestone, 2: thick heavily fractured black limestone. Joints are filled calcite.

Outcrop III, presumably Ravdoucha beds. Thin black limestone and black slate beds.

Outcrop IV, massive dark grey Tripoliza limestone overlying the Ravdoucha beds at east side of the valley

9.4 Tripoliza Limestone

Outcrop V, finely bedded grey Tripoliza limestone at west side of the valley. Many of the beds are ocher coloured probably owing to small amounts of hydrated iron hydroxide [limonite, $FeO(OH)\cdot nH_2O$]

Outcrop VI, small cliff face at the west side of the valley. The Tripoliza limestone is covered

with travertine forming stalactite structures. Travertine is a sedimentary rock formed by the chemical precipitation of calcium carbonate minerals from fresh water, typically in springs, rivers, and lakes; that is, from surface and ground waters. At one time, probably during the Quaternary, carbonate rich water must have continually flowed over the edge of the ridge.

10 Mariou to Asamatos

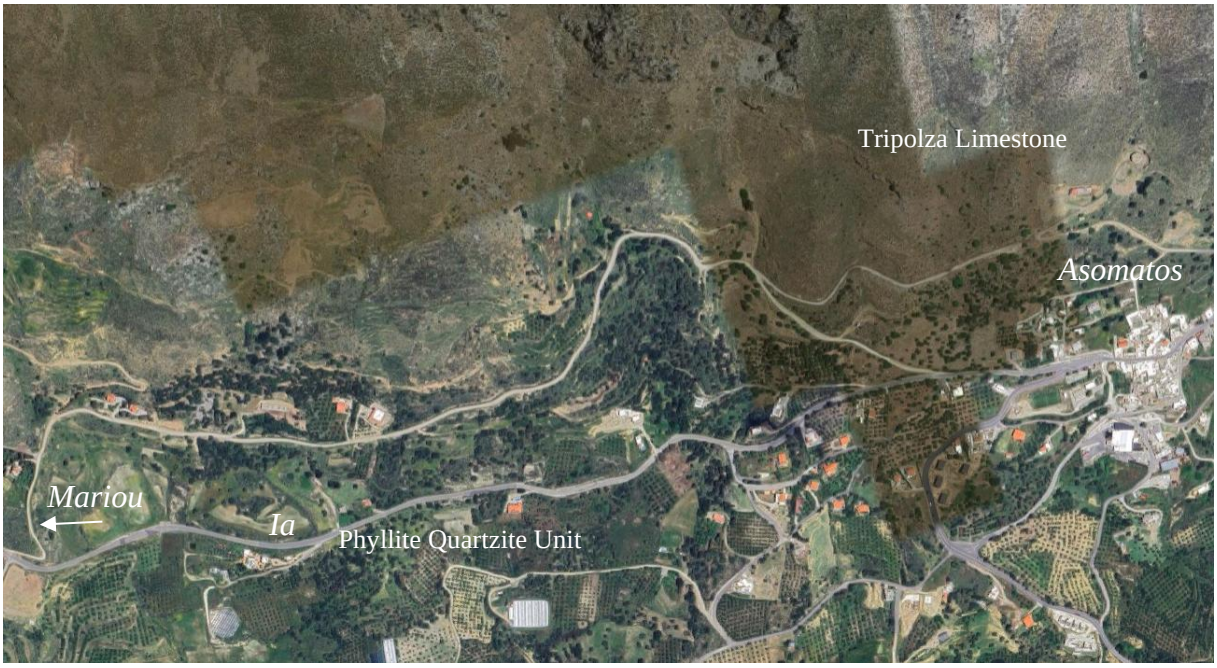

Location of outcrops near Asomatos [source of image : Google Maps]

Outcrop Ia: Phyllite-Quartzite unit

Outcrop Ia: Phyllite-Quartzite unit displaying predominantly phyllite rock.

References

Alexandra van der Geer1 & George Lyras, 2011: Field Trip Guidebook European Association of Vertebrate Palaeontologists, 9th Annual Meeting Heraklion, Crete, Greece 14-19 June, 2011

Alves, T. Cupkovic T., 2018: Footwall degradation styles and associated sedimentary facies distribution in SE Crete: Insights into tilt-block extensional basins on continental margins; 3D Seismic Lab, School of Earth and Ocean Sciences, Cardiff University, Cardiff, United Kingdom; Husky Energy, Atlantic Region, 351 Water St., Suite 105, St. John's, Canada

Brack P., Meister P. H., Bernasconi S., 2013: Dolomite formation in the shallow seas of the Alpine Triassic, Article in Sedimentology · Feb. 2013, DOI: 10.1111/sed.12001]

Brandes C. et al., 2014: Fault-related folding: A review of kinematic models and their application, Institute for Geology, Leibniz Universität Hannover, Callinstr. 30, 30167 Hannover, Germany

Champod E. et al., 2010: Stampfli Field Course: Tectonostratigraphy and Plate Tectonics of Crete, Université de Lausanne, September 2010

Chatzaras, v., Xypolias, P. & Doutsos, T (2006): Exhumation of high-pressure rocks under continuous compression: a working hypothesis for the southern Hellenides (central Crete. Greece). - Geol. Mag. 143: 859-R76.

Fassoulas C., 2000: The tectonic development of a Neogene basin at the leading edge of the active European margin: the Heraklion basin, Crete, Greece, Natural History Museum of Crete, University of Crete, Heraklion 71409, Greece

Fassoulas C., Rahl J.M., 2004: Patterns and Conditions of Deformation in the Plattenkalk Nappe, Crete, Greece: A Preliminary Study, Natural History Museum of Crete, Yale University, New Haven, Connecticut

Granger D.E., 2007: Cosmogenic Nuclide Dating - Landscape Evolution, in Encyclopedia of Quaternary Science, Pages 445-452

Kull U., 2012: Kreta, Sammlung geologischer Führer

McClay K.R.: Glossary of thrust tectonics terms, Department of Geology, Royal Holloway and Bedford New College, University of London, Egham, Surrey, England

Miller W., 1977: Geologie des Gebites Nördlich des Plakias-Bucht, Kreta, Freiburg im Breisgau, Diplomarbeit

Mountrakis D., Kilias A., Pavlaki A., Fassoulas C., Thomaidou E., Papazachos C., Papaioannou C., Roumelioti Z., et al., 2012: Neotectonic study of Western Crete and implications for seismic hazard assessment, Journal of the Virtual Explorer, Electronic Edition, ISSN 1441-8142, volume 42, paper 2 In: (Eds.) Emmanuel Skourtsos and Gordon S. Lister, The Geology of Greece, 2012.

Pirazzoli P.A., Thommeret J., Thommeret Y., Laborel J., and Montaggioni L.F., 1982: Tectonophysics 86, 27-43.

Pomoni F., Karakitsios V., 2016: Sedimentary facies analysis of a high-frequency, small-scale, peritidal carbonate sequence in the Lower Jurassic of the Tripolis carbonate unit (central western Crete, Greece): Long-lasting emergence and fossil laminar dolocretes horizons, Department of Geology and Geoenvironment, National and Kapodistrian University of Athens

Rahl J. M. et. al.: Exhumation of high-pressure metamorphic rocks within an active convergent margin, Crete, Greece: A field guide, Jeffrey M. Rahl, Charalampos, Fassoulas, and Mark T. Brandon, Department of Geology and Geophysics, Yale University, New Haven, Connecticut 06511, U.S.A. Natural History Museum of Crete, University of Crete, Heraklion 71409, Greece

Rieger S., 2015: Regional-Scale, Natural Persistent Scatterer Interferometry, Island of Crete (Greece), and Comparison to Vertical Surface Deformation on the Millennial-, and Million-Year Time-Scales; Phd.; Ludwig-Maximilians-Universität München

Seidel M., 2003: Tectono-sedimentary evolution of middle Miocene supra-detachment basins (western Crete, Greece), Ph.D. Dissertation, University of Köln.

Stampfli 2010: Stampfli Field Course, Tectonostratigraphy and Plate Tectonics of Crete, Université de Lausanne, France

Steiakakis E., 2017: Evaluation of Exploitable Groundwater Reserves in Karst Terrain: A Case Study from Crete; Greece Laboratory of Applied Geology, Technical University of Crete, 73100 Chania, Greece

Thomson S. N. et al., 1989: Apatite fission-track thermochronology of the uppermost tectonic unit of Crete, Implications for the post-Eocene tectonic evolution of the Hellenic Subduction System, Institut für Geologie, Ruhr-Universität Bochum

Thomson S. N., Stockert B., Brix M. R., 1999. Miocene high-pressure metamorphic rocks of Crete, Greece: rapid exhumation by buoyant escape. In: Ring, U., Brandon M. T., Lister G. S., Willetf S. D. (eds): Exhumation Processes: Normal Faulting, Ductile Flow and Erosion. Geological Society, London, Special Publications, 154, 87-107.

Thomson S. N., Stockhert, B. & Brix, M.R. (1998a): Thennochronology of the high-pressure metamorphic rocks of Crete, Greece: implications for the speed of tectonic processes. - Geology 26: 259-262.

Thrust faults: Some common terminology - Geological Digressions https://www.geological-digressions.com

Tiberti M. M., Basili R. & Vannoli P., 2014: Ups and downs in western Crete (Hellenic subduction zone), Istituto Nazionale di Geofisica e Vulcanologia, Via di Vigna Murata 605, 00143 Rome, Italy

van Hinsbergen D. J. J., Meulenkamp J. E., 2006: Neogene supradetachment basin development on Crete (Greece) during exhumation of the South Aegean core complex.

Vassilakis E. and Alexopoulos J., 2012: Recognition of Strike-slip Faulting on the Supradetachment Basin of Messara (Central Crete) with remote sensensing Image Interpretation Techniques; National and Kapodistrian University, Department of Dynamics,

Tectonics and Applied Geology, Athens, Greece; National and Kapodistrian University, Department of Geophysics & Geothermics, Athens, Greece;

Wassmann S., 2012 Geländekurs Kreta

Zachariasse W., van Hinsbergen D., et al. 2011, Formation and Fragmentation of a late Miocene supradetachment basin in central Crete: implications for exhumation mechanisms of high-pressure rocks in the Aegean forearc, Stratigraphy and Paleontology group, Faculty of Geosciences, Utrecht University, Utrecht, The Netherlands; Physics of Geological Processes, University of Oslo

11 Appendix

Geological Time Scale

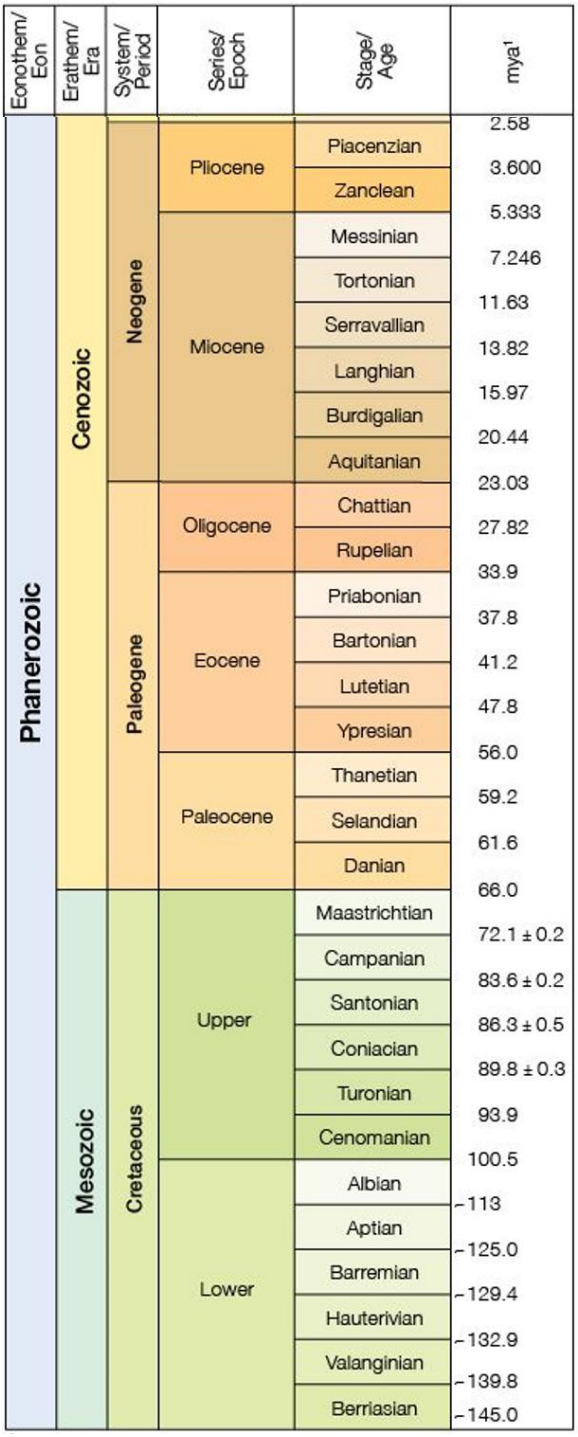

Eonothem/ Eon	Erathem/ Era	System/ Period	Series/ Epoch	Stage/ Age	mya[1]
Phanerozoic	Cenozoic	Neogene	Pliocene	Piacenzian	2.58
				Zanclean	3.600
			Miocene	Messinian	5.333
				Tortonian	7.246
				Serravallian	11.63
				Langhian	13.82
				Burdigalian	15.97
				Aquitanian	20.44
		Paleogene	Oligocene	Chattian	23.03
				Rupelian	27.82
			Eocene	Priabonian	33.9
				Bartonian	37.8
				Lutetian	41.2
				Ypresian	47.8
			Paleocene	Thanetian	56.0
				Selandian	59.2
				Danian	61.6
	Mesozoic	Cretaceous	Upper	Maastrichtian	66.0
				Campanian	72.1 ± 0.2
				Santonian	83.6 ± 0.2
				Coniacian	86.3 ± 0.5
				Turonian	89.8 ± 0.3
				Cenomanian	93.9
			Lower	Albian	100.5
				Aptian	~113
				Barremian	~125.0
				Hauterivian	~129.4
				Valanginian	~132.9
				Berriasian	~139.8
					~145.0

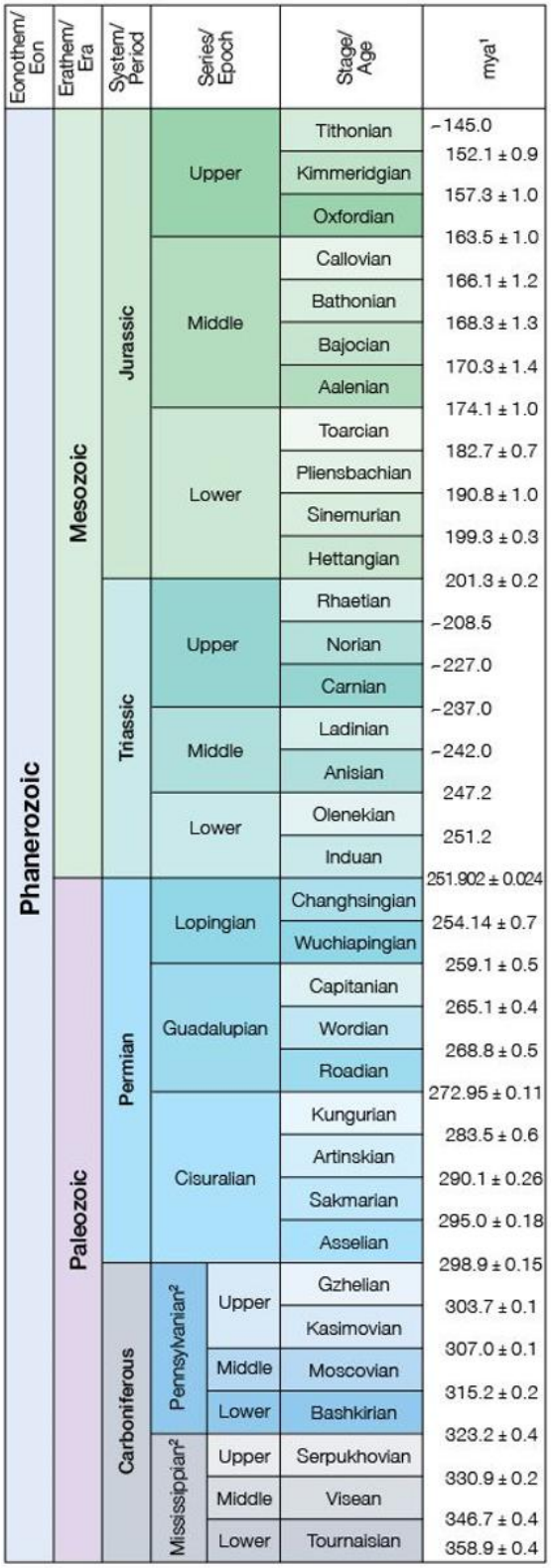

Eonothem/ Eon	Erathem/ Era	System/ Period	Series/ Epoch		Stage/ Age	mya[1]
Phanerozoic	Mesozoic	Jurassic	Upper		Tithonian	~145.0
					Kimmeridgian	152.1 ± 0.9
					Oxfordian	157.3 ± 1.0
			Middle		Callovian	163.5 ± 1.0
					Bathonian	166.1 ± 1.2
					Bajocian	168.3 ± 1.3
					Aalenian	170.3 ± 1.4
			Lower		Toarcian	174.1 ± 1.0
					Pliensbachian	182.7 ± 0.7
					Sinemurian	190.8 ± 1.0
					Hettangian	199.3 ± 0.3
		Triassic	Upper		Rhaetian	201.3 ± 0.2
					Norian	~208.5
					Carnian	~227.0
			Middle		Ladinian	~237.0
					Anisian	~242.0
			Lower		Olenekian	247.2
					Induan	251.2
	Paleozoic	Permian	Lopingian		Changhsingian	251.902 ± 0.024
					Wuchiapingian	254.14 ± 0.7
			Guadalupian		Capitanian	259.1 ± 0.5
					Wordian	265.1 ± 0.4
					Roadian	268.8 ± 0.5
			Cisuralian		Kungurian	272.95 ± 0.11
					Artinskian	283.5 ± 0.6
					Sakmarian	290.1 ± 0.26
					Asselian	295.0 ± 0.18
		Carboniferous	Pennsylvanian[2]	Upper	Gzhelian	298.9 ± 0.15
					Kasimovian	303.7 ± 0.1
				Middle	Moscovian	307.0 ± 0.1
				Lower	Bashkirian	315.2 ± 0.2
			Mississippian[2]	Upper	Serpukhovian	323.2 ± 0.4
				Middle	Visean	330.9 ± 0.2
				Lower	Tournaisian	346.7 ± 0.4
						358.9 ± 0.4

Strain Ellipsoid and Flinn's Diagram

Strain in 2D - the strain ellipse

Deformation is caused by forces acting on the rock body. These forces maybe due to gravity (vertical force) or the movement of the tectonic plates (horizontal forces). The effect of these forces on a rock depends on the area over which they are applied: force/area=stress. Therefore, at its simplest, stress causes strain. Depending on lithospheric conditions at the time of deformation, rocks may respond to stress in a brittle or ductile manner. During brittle deformation rocks fracture with strain localised along a plane whilst the rocks to either side remaining unaffected (e.g. faults and joints). During ductile deformation rocks change shape smoothly and strain is pervasive throughout the rock body (e.g. folds) *[Introduction to structural geology, Workbook 1 Structural Geology - the Basics, University of Leeds]*

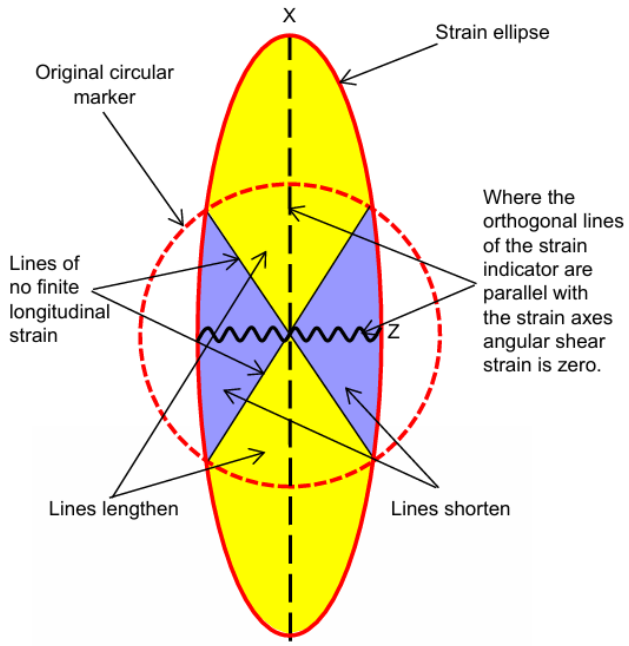

Figure 9: The strain ellipse.

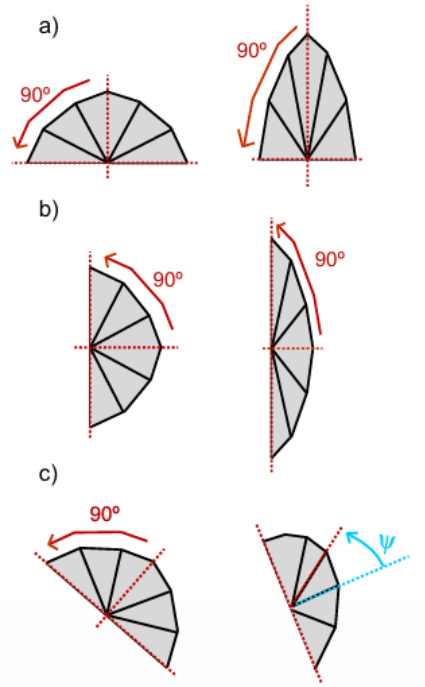

Figure 10: Fossils a) and b) have their orthogonal lines parallel with the strain axes and show no shear strain during deformation. Fossil c) is at an angle to the strain axes and shows shear strain during deformation.

The strain ellipse is a method of representing the amount of strain a rock has undergone. It uses an initially circular marker that is deformed to an ellipse (figure 9). The strain ellipsoid is used for strain in three dimensions. The value of longitudinal strain depends on original orientation of a line. Lines that are parallel or close to parallel with the Z axis will contract, lines that are parallel or close to parallel with the X axis will elongated and lines that are parallel or close to parallel to the lines of no finite longitudinal strain will undergo contraction followed by elongation. The lines of no finite longitudinal strain separate the zone of elongation (yellow) from the zone of contraction (blue). The value/sense of angular shear strain depends on original orientation of the orthogonal lines of the strain indicator. Where the lines of the strain indicator

are parallel with the strain axes (X and Z) shear strain is zero. Where they are at an angular shear strain occurs (figure 10).

Strain in 3D

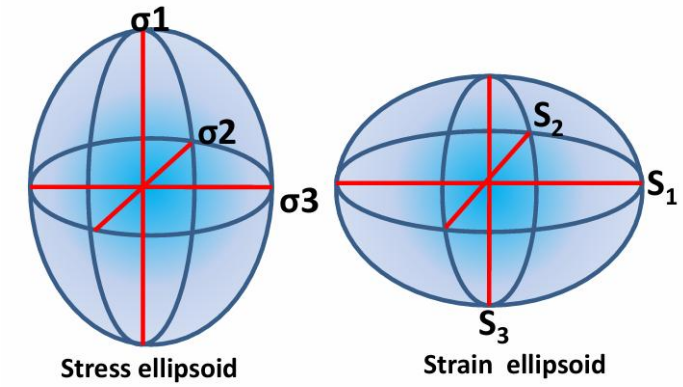

Relationship between stress and strain ellipsoid

Difference between Stress and Strain ellipsoid

The relation is exactly opposite between these ellipsoids in respect to the position of greatest and least principal axis.

Strain ellipsoid represents the effect of deformative forces applied on the body of rock.

With the help of deformation in rocks we can construct the strain ellipsoid, from strain ellipsoid and with other evidences orientation of stress ellipsoid can be drawn.

The Flinn diagram is a graphical representation used to plot diagram finite strain ellipsoids. The Flinn diagram describes two main types of strain ellipsoids, cigar and pancake. S3 S2 a = S1/S2 b = S2/S3 K = a-1/b-1

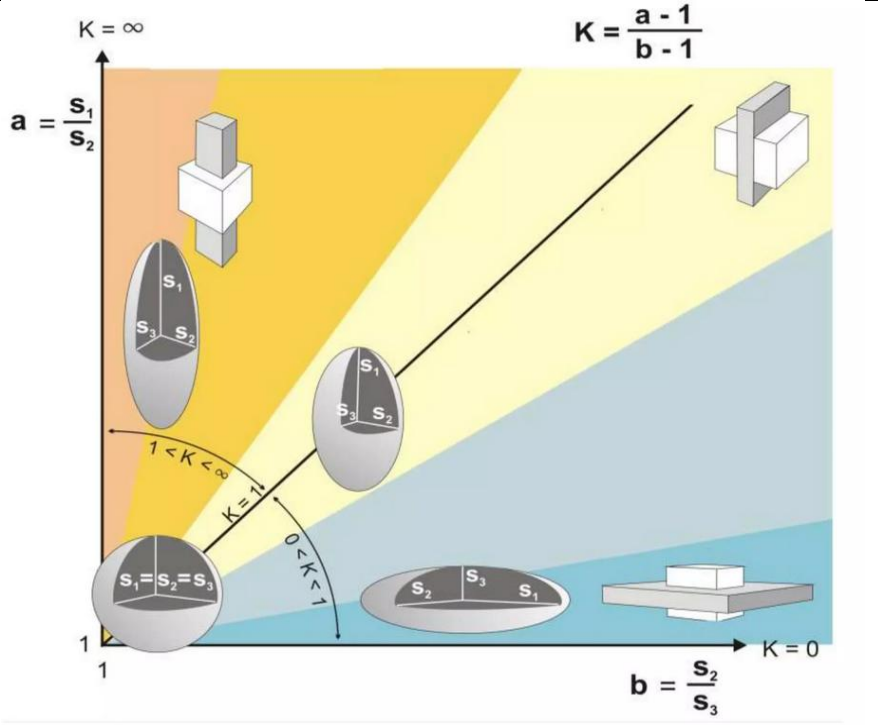

a = S1/S2 b = S2/S3 K = a-1/b-1

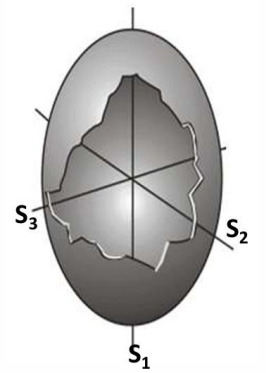

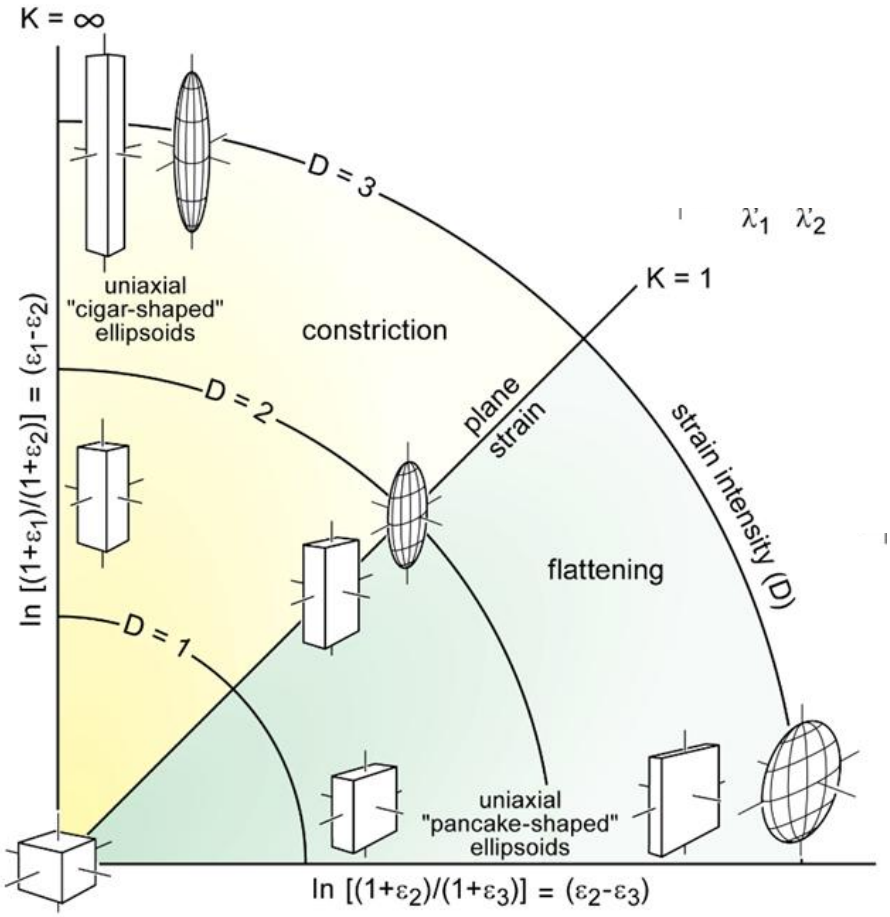

Source: Finite strain (jpd 2020)

K=∞	**Axially symmetric stretching**; XYZ>>>>≥; Ellipsoids have a long, cigar shape and plot near the vertical: axis.
∞ >K> 1	**Constrictional strain**; in this case, X>Y =Z ; the ellipsoids have a prolate to cigar shape and plot near the vertical axis, above the plane strain line.
K1	**Plane strain** at constant volume.
1>K> 0	**Flattening strain**; in this case, X=Y>Z ; the ellipsoids have an oblate to pancake shape and plot below the diagonal line, near the horizontal axis.
K0	**Axially symmetric flattening**. XYZ≥>>>> The flat ellipsoids plot along the horizontal axis

Coaxial vs Non-coaxial shear

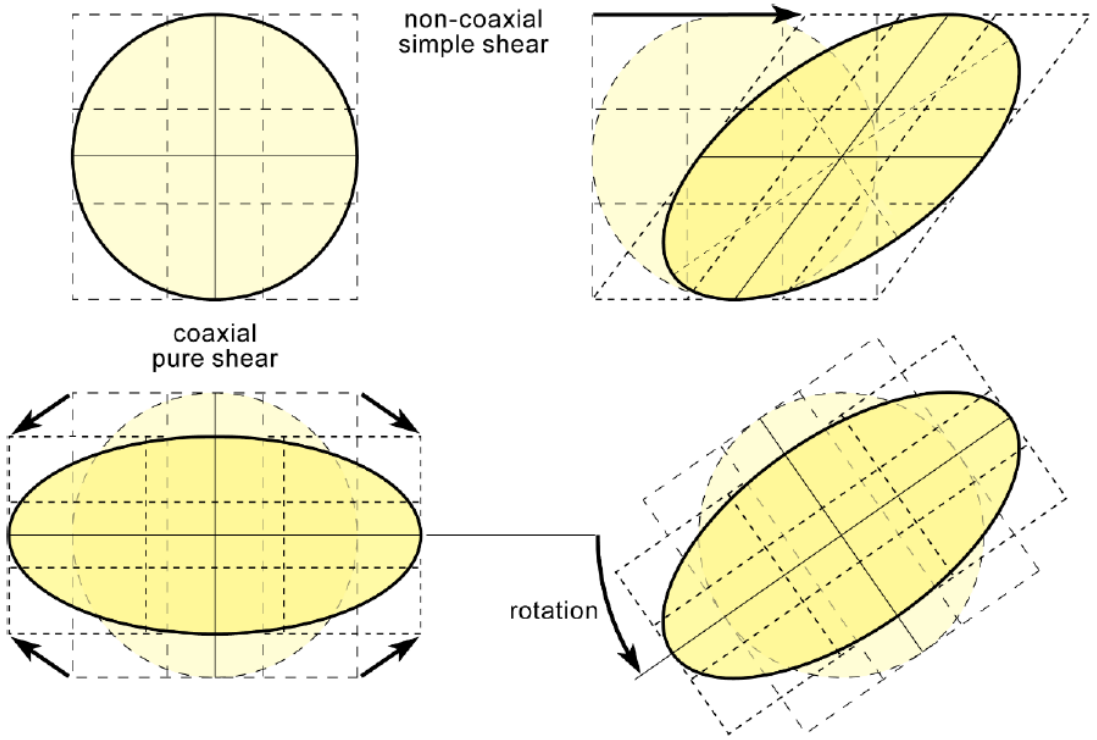

Source: Finite strain (jpd 2020)

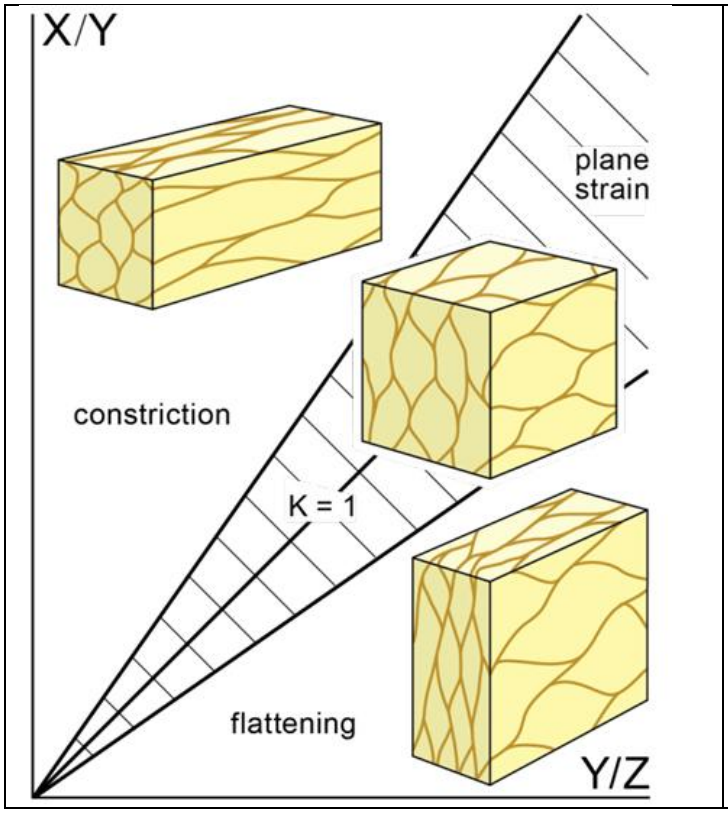

Array of shear zones with respect to bulk strain regime (Gapais et. al. 1987)

Thrust Faults

Stages of thrust development in a sandbox experiment. First image: two thrusts and associated fault propagation folds, after about 31% horizontal shortening. Second image: Greater complexity after 56% shortening. The beginning of a new thrust is also apparent at the frontal edge of the "thrust belt". [Prof. Sandra McLaren, Melbourne University, Twitter page @sandramcgeo]. Thrust faults: Some common terminology - Geological Digressions https://www.geological-digressions.com

Sand box and critical taper theory

[Jpd Tectonics, 2017: Thrust Systems]

The mechanical development of folds-and-thrusts-belts is compared to the piling up of loose sand in front of a bulldozer as it is pushed up a slope.

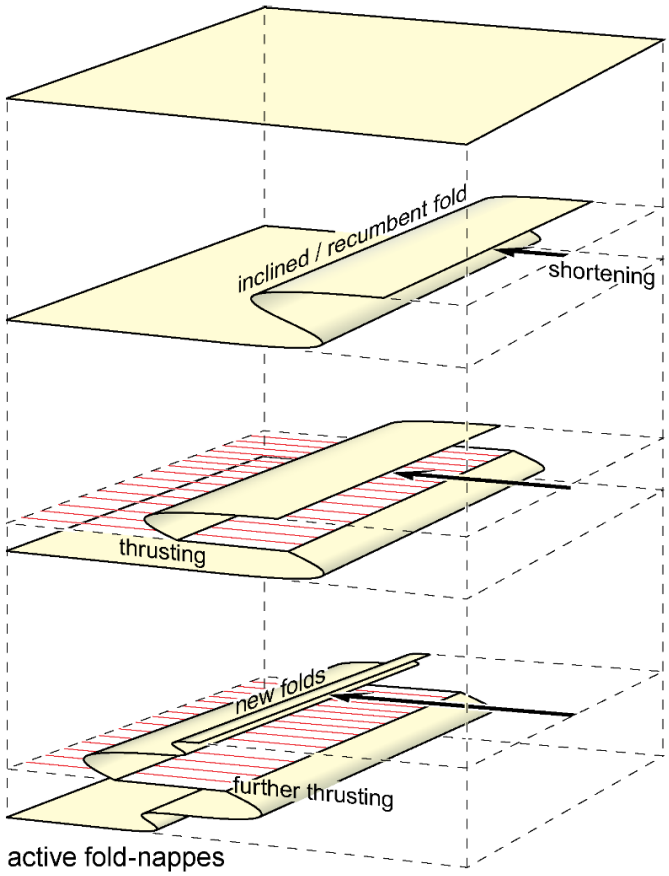

Active folds

Active folding means either that folding and thrusting processes are coeval or that folding absorbs some shortening before thrust activation. These two possibilities largely depend on the metamorphic conditions. At low temperature and pressure conditions (i.e. within the sub-surface crust) thrust-related folds are passive. Shortening strain becomes progressively more ductile with depth, i.e. folding becomes more important.

Stretched-fold thrusts (fold nappes)

The concept has been developed in the Alps by the beginning of the 20th century. The ductile, overturned limb of a growing fold stretches and thins down until it breaks into a thrust.

Geological application

A geological wedge is believed to evolve by the addition of sediment scrapped at its toe from the down-going slab. In support, seismic profiles across convergent mountain systems frequently show that a major décollement separates the colliding plates. Large amounts of subhorizontal motion take place on this décollement, also known as sole thrust (or basal thrust), which dips gently towards the overriding plate. Motion along the décollement results in the tectonic accretion of imbricate slices one on top of the next in the deforming hanging wall through distributed horizontal shortening as well as folding and faulting.

- The hanging wall develops into a wedge-shaped tectonic unit, when viewed in cross-section parallel to the movement direction, with the narrow end in the direction of motion.
- The subducting footwall, however, remains relatively undeformed, which typifies a thin-skinned thrust belt.

Moving thrust wedges are driven by plate convergence but the geometry acts in response to the rate of convergence and to the strength of the basal detachment. Hence, they are in a state of dynamic equilibrium. The sole thrust is considered to be weak while the wedge material follows the Mohr-Coulomb failure criterion. The corresponding Mohr construction implies that rocks effectively increase in strength as lithostatic pressure rises; hence the rocks at the back end of the wedge are effectively stronger than those at the front. Variants of wedge models have ncorporated a number of different types of rheology. The wedge models link the topography of orogenic belts to the rheology of the crust and includes the effects of body forces and externally applied tectonic forces.

Fault-related folding

Brandes C. et al., 2014

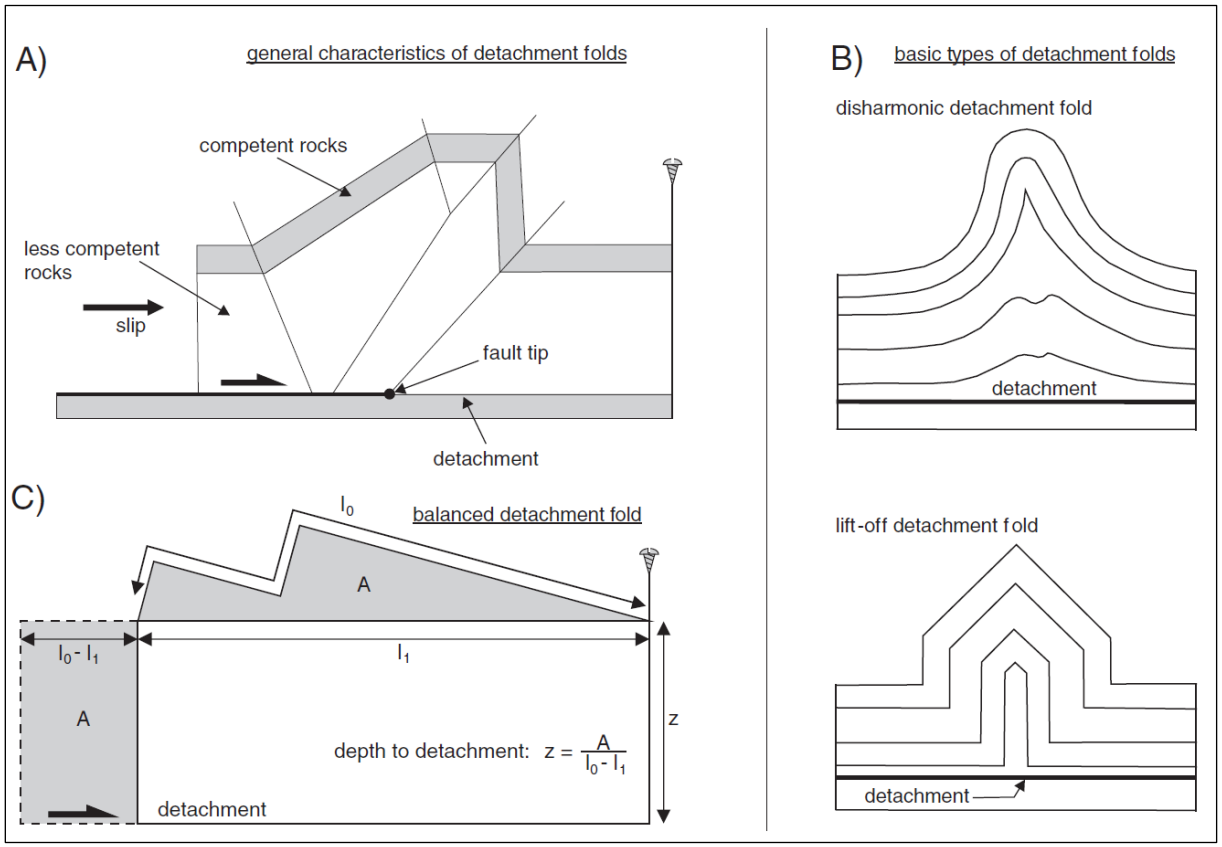

Fig. 6. Detachment folds. A) General characteristics of detachment folds are a horizontal detachment and a core of less-competent rocks. B) Types of detachment folds: 1. fold core is characterized by disharmonic folds, 2. Lift-off folds, where the core is characterized by isoclinal limbs. C) Depth-to-detachment calculation of a detachment fold, using the excess-area-method.

Kinematic models

The sense of shear along the fault can be determined by the asymmetry of the drag fold. Furthermore, the slip vector can be estimated using Hansen's Method (Hansen, 1971; Twiss and Moores, 1992). If the fold is conical, then the fold axis is the axis of rotation of the beds at the fault, which is perpendicular to the slip direction (Becker, 1995). Recently, numerical (finite element) models have been used to test drag folding geometries and processes (e.g. Reches and Eidelman, 1995; Resor and Pollard, 2012). These models prove that edge dislocation in an

elastic half space is sufficient to produce the majority drag folds, and that friction on the fault is not important.

Detachment folds

Detachment folds are folds that evolve from the shortening of a rock mass above either a detachment or a décollement (e.g. Poblet et al., 1997; Rowan, 1997; Scharer et al., 2004; Poblet and Hardy, 1995) (Fig. 6A). A detachment is defined as a low-angle fault that may be nearly, but not exactly parallel to a horizon, whereas as a décollement is a bedding- or layer-parallel fault (Peacock et al., 2000). Detachment folds also develop above the tip of a bedding-parallel thrust (Poblet and McClay, 1996) in competent rocks and are often cored by less competent rocks (Homza and Wallace, 1995). Distinct detachment folds can only form if there is enough mobile material present in the detachment layer to fill the core of the growing anticline (Stewart, 1996). If there is not enough material to fill the amplifying fold, fold growth will stop and shortening may be compensated by faulting (Stewart, 1996).

The most important characteristic feature of detachment folds is the detachment horizon (i.e. décollement) (Fig. 6A) that is developed either above, below, or above and below the fold. Layer-parallel strain allows the fold to develop above a fixed stratigraphic detachment (Groshong and Epard, 1994). Detachment folds are often symmetric (Hardy and Finch, 2005) and their geometries range from concentric to chevron type folds or even box folds (Rowan et al., 2004; Shaw et al., 2005). Internally, detachment folds are characterized by homogeneous strain, second-order folds, second-order conjugate faults, or duplex structures (Epard and Groshong, 1995). Detachment folds can be subdivided into two main groups: a) disharmonic folds and b) lift-off folds (Mitra and Namson, 1989). Disharmonic folds are parallel or concentric folds with disharmonic folding in the core (Fig. 6B). Lift-off folds are parallel folds, where the core of the anticline is characterized by isoclinal limbs (Fig. 6B). Early models of detachment folds were geometrical (Jamison, 1987) that focused on the shape of the folds. Different kinematic models were developed later. From an area-balanced cross-section it is possible to derive the
depth of the detachment (Fig. 6C).

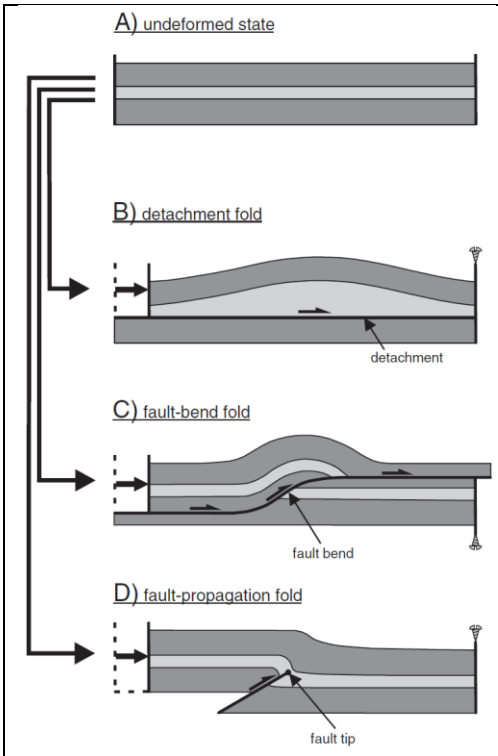

Fig. 2. The three main types of fault-related folds. A) Undeformed state. B) A detachment fold evolves from the shortening of a rock mass above a detachment. The space in the fold core is filled with mobile material. C) A fault-bend fold forms when material is transported over a bend in a fault. This forces the material into an antiformal geometry. D) Fault propagation folds form as a consequence of variation in the slip along the fault. The slip on a fault is assumed to decrease to zero at the tip, which is compensated by buckling of material above the fault.

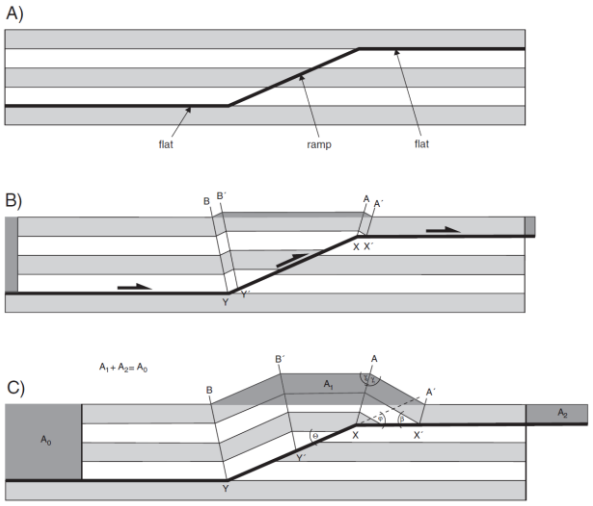

Fig. 7. Kink-band migration model for a fault bend fold, based on Suppe (1983). Material is transported over a footwall ramp and deformed into an antiform, see text for explanation.

Fault-bend folds

Fault-bend folds occur when material is transported over a thrust footwall ramp (Berger and Johnson, 1980), i.e. a steepening of the fault plane that typically crosscuts stratigraphy rather than following the bedding plane (Suppe, 1983) (Fig. 2C). This concept was originally introduced by Rich (1934) based on his observations in the Appalachians. Wiltschko (1979) developed a mechanical model for a thrust sheet that moves over a ramp. Fault-bend faults have been recognized in fold-and-thrust belts all over the world and have been the focus of many studies (Suppe, 1983; Zoetemeijer et al., 1992; Medwedeff and
Suppe, 1997; Savage and Cooke, 2003; Suppe et al., 2004).

The basic requirements for the evolution of fault-bend folds are changes in the geometry of the fault plane, such as bends or ramps. A footwall ramp usually connects two horizontal detachments (flats) at

different stratigraphic levels (Fig. 7). By moving from the first, deepest footwall flat to the shallowest, the hanging-wall material will be deformed into a syncline–anticline–syncline structure. Another requirement for fault-bend folding is that the fault blocks are in tight contact along the plane and the bend in the fault does not lead to the development of significant voids (Suppe, 1983). In the case of fault-bend folds, the propagation rate of the fault must be much higher than fault slip, because the fold forms before the first increment of slip (McNaught and Mitra, 1993). Bending of the material during the transport over the ramp is accommodated by bedding-parallel simple shear and the magnitude of shear strains is related to the ramp angle (Sanderson, 1982). This causes beds to thin over a concave fault bend. To produce a fault-bend fault, enough energy must be available to overcome the friction on the fault, uplift the fold, and shear the fold material (Williams, 1987).

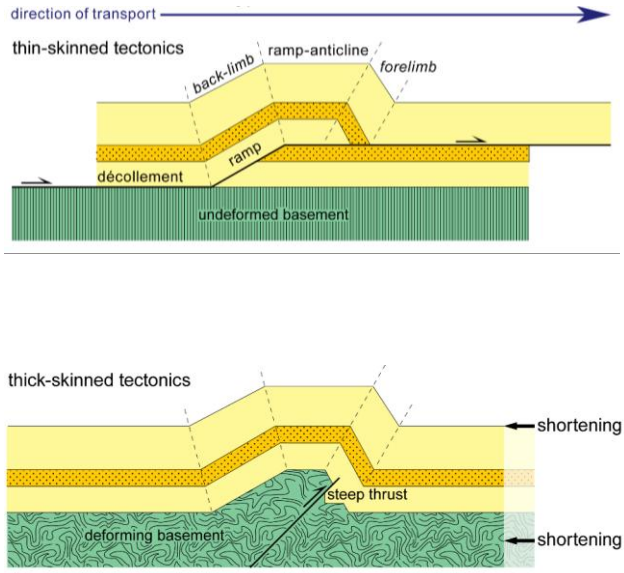

Thin and Thick-Skinned Tectonics [Jpd Tectonics, 2017: Thrust Systems]

Thin-skinned tectonics principally refers to thrusting that does not affect the basement whereas subparallel sets of folds and faults deform the cover. The initially sub-horizontal sedimentary sequence is detached along weak décollement horizons (e.g. salt, shale, over pressured layers) and is deformed independently from the underlying substratum. Typically, deformation is confined to the cover while the basement slides underneath rigidly (no thrust cuts through).

Thick-skinned tectonics
In hinterlands, often the crystalline core-axes of mountain belts, deformation is principally controlled by high-angle thrusts and their interaction with the deforming ductile basement. Thrusting that involves basement deformation is termed thick-skinned tectonics. Combined basement-cover thrust sheets are designated as basement-cored nappes.

[Jpd Tectonics, 2017: Thrust Systems]

Duplex structures

Thrust systems commonly involve several approximately parallel décollement-surfaces whose location and extent are controlled by weak layers at different levels of a sedimentary pile. A thrust-duplex consists of a series of sub-parallel ramps that branch off a relatively flat, lower floor thrust (also called sole thrust) and merge upward into the upper roof thrust. The whole structure encloses a package of S-shaped, detached slices of rock stacked in a systematic manner. The individual imbricate lenses are called imbricates or horses. Typically, horses make a progressively larger angles with the roof- and floor-faults from front to back (like in leading fans). Unlike an imbricate fan, a thrust duplex is contained within the sedimentary sequence.

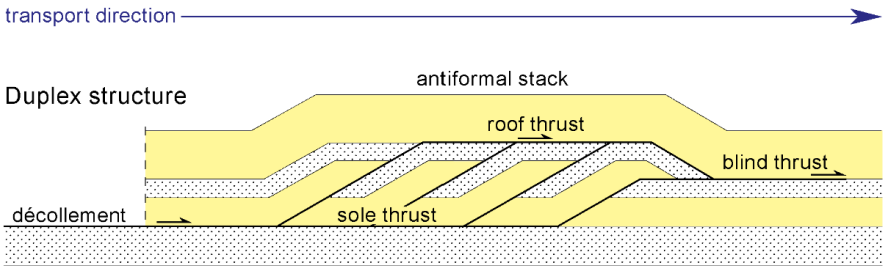

Duplex formation is initiated when the forward propagation of a thrust is impeded by some perturbation or sticking point. The thrust is forced to ramp up to a higher glide horizon. With continued displacement on the thrust, higher stresses are developed in the footwall of the ramp, which makes an obstacle to the horizontal movement of rocks. Increased stresses cause renewed propagation of the floor thrust ahead of the ramp along the décollement horizon, until the fault plane again cuts up to join the roof thrust. Further displacement then takes place along the newly created ramp. This process may repeat many times, forming a series of fault bounded, typically a lozenge shaped horses. The tectonic shift of the footwall ramp by the sequential formation of thrust slices creates the duplex structure. The development of each new thrust slice is accompanied by the backward rotation and 'piggy-back' transport of the earlier-formed horses. Parameters that determine the final geometry of the duplex include the ramp angle, the initial and final spacing of the thrusts, and the amount of displacement on them. *[Jpd Tectonics, 2017: Thrust Systems]*

Carbonate Platform Facies

Miocene syn-rift carbonate–siliciclastic rock packages, Gulf of Suez, Egypt

Inner Ramp

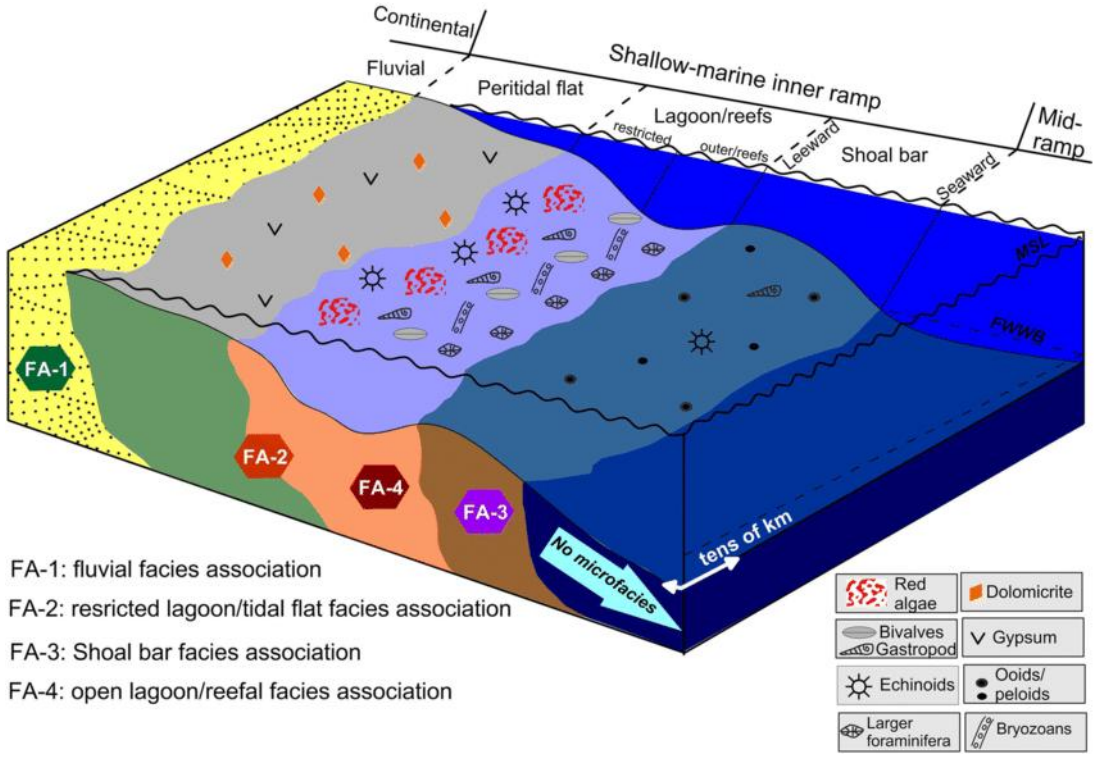

Source: Sallam, E.S., Ruban, D.A. Facies analysis and depositional environments of the Miocene syn-rift carbonate–siliciclastic rock packages in the northwest Gulf of Suez, Egypt, Carbonates Evaporites 35, 10 (2020). https://doi.org/10.1007/s13146-019-00547-7

The Miocene sedimentary successions in the northwest Gulf of Suez allow insight into the syn-rift deposition. These rocks are subdivided into three formations, namely the Sadat Formation coeval with the Gharra Formation (Early Miocene), the Hommath Formation (Middle Miocene), and the Hagul Formation (Late Miocene). The Miocene rocks in the study area are dominated by carbonate-siliciclastic packages. Detailed microfacies analysis permit discrimination of 14 sedimentary microfacies types, which are represented by continental quartz-arenites and sandy siltstones, as well as shallow-marine gypsiferous laminated shales, litharenites, dolomicrites, wackestones, wacke-/packstones, packestones, pack-/grainstones, ooidal/pelloidal pack-/grainstones, grainstones, rudstones, framestones, and bindstones. These microfacies types are stacked into four facies associations that represent fluvial, and inner ramp, shallow marine environments (facies associations for the later are restricted lagoonal/tidal flat, shoal bar, and open-lagoonal/reefal). In terms of sequence stratigraphy, it is possible to distinguish five depositional sequences in the studied Miocene succession. The retrogradational package displays predominance of open lagoon/reefal facies. The aggradational package shows increase in restricted lagoon tidal flat and shoal bar facies. The progradational package marks occurrence of continental (fluvial) facies. The regional tectonic activity related to the rifting of the Gulf of Suez was the leading control of the Miocene sedimentation in the study area.

Miocene carbonate ramp development in a warm ocean, North West Shelf, Australia

Rosine Riera, Julien Bourget, Tony Allan, Eckart Håkansson, Moyra E. J. Wilson

https://onlinelibrary.wiley.com/doi/full/10.1111/sed.12917

Mid ramp to outer ramp

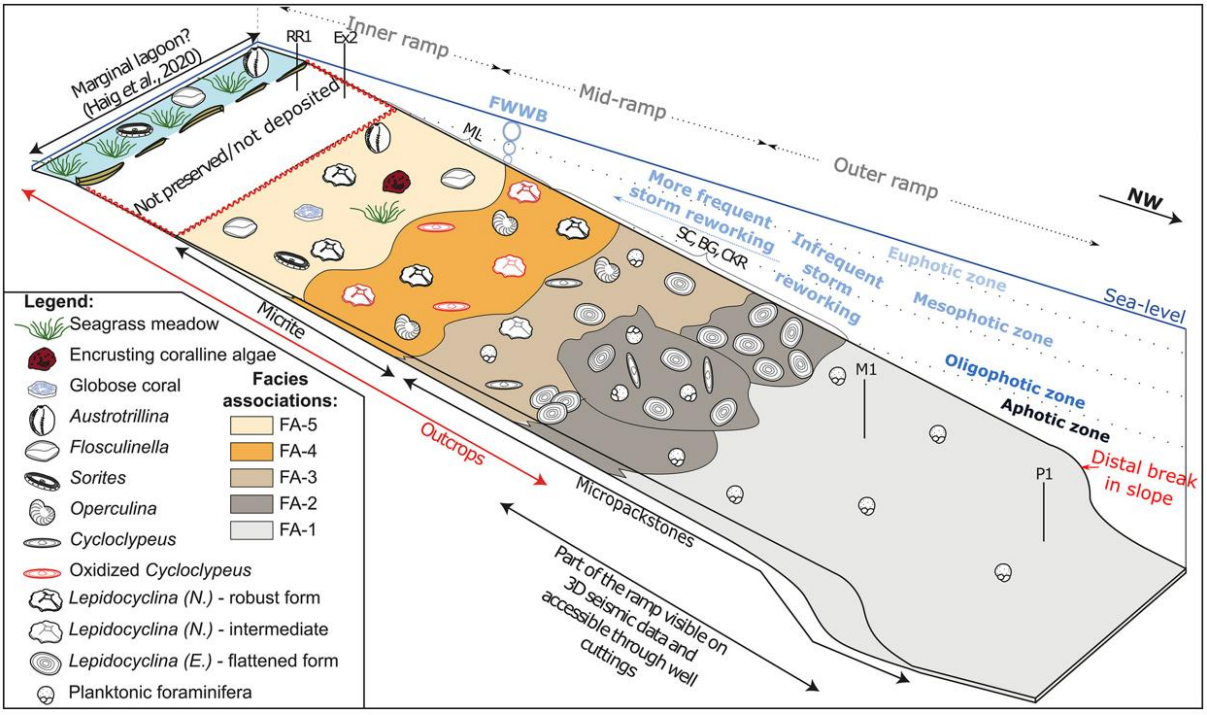

Abstract

Although carbonate ramps are widely described from the geological record, there is still a debate on the relative influence of water temperature, trophic conditions and type of carbonate factories on their development. The ca 2400 km long Australian North West Shelf is among the largest Cenozoic carbonate provinces worldwide, and records a transition from an early Miocene ramp to a middle Miocene rimmed platform. This change is observable on publicly available seismic data, giving the opportunity to investigate environmental influences on platform evolution. This study combines macroscopic and petrographic descriptions of early Miocene strata cropping out in the Cape Range Anticline (North West Cape, southern end of the North West Shelf) and of time-equivalent well cuttings from the adjacent, offshore Exmouth Sub-basin. Particular emphasis is placed on the identification of larger benthic foraminifera at a broad generic level, because differing taxa have a limited range of habitable conditions that serve as environmental proxies. The results show that early Miocene strata are dominantly composed of larger benthic foraminifera with minor coralline algae in the proximal platform, grading to micropackstones in the more distal platform. A ramp margin is inferred from the lithological data on the basis of the lack of framework builders and the presence of open oceanic indicators. Facies shallow upward through individual outcrops, with a proximal to distal trend towards the north-west. These trends along outcrops are consistent with the seismic interpretations. Identification of taxa with warm, oligotrophic water affinity suggests that the ramp was formed in an oligotrophic and warm ocean, despite the absence of coral reefs. Changes of carbonate facies with depth do not seem to be associated with changes in ramp

morphology, and the latter may have been controlled by physical oceanic parameters, such as offshore currents and waves.

Dolomite

Dolomit sample from the Triassic of the Slovakian Carpathians. Notice the slightly brown colour and splintery rock surface

Dolomite is somewhat harder and much more brittle than the chemically related limestone with a similar structure and texture. Like limestones, dolomites are often grey on fresh fracture surfaces, but usually weather to a yellowish or brownish color. The first indication of dolomite in the outcrop is a rather splintery rock surface. The lack of smoothly weathered /washed surfaces is in contrast to limestone. In the field, dolomite can also be distinguished from limestone by its very slow reaction with cold, diluted (10 percent) hydrochloric acid: With dolomite, virtually no carbon dioxide bubbles develop after the hydrochloric acid is applied, whereas with limestone the acid reacts vigorously. Due to its lower susceptibility to dissolution by weak acids, dolomite karstifies to a lesser extent and differently to limestone. To detect the presents of dolomite in a carbonate rock sample, the rock can be treated with chinalizarin, which reacts with Mg and colours dolomite pink.

In literature dolomite is often refers to as having a “sugar-grained” appearance. This refers to the structure of fine crystals, which are much finer-grained than the commercial sugar commonly used today, but coarser-grained than limestone crystals. The cleavage surfaces glisten visibly in sunlight. This fine crystallinity can be attributed to recrystallization during or shortly after sedimentation. If dolomitization occurs in the early diagenetic stage, structural features and fossils remain intact. Late diagenetic dolomitization obliterates any structural

features and fossils of the original rock. Therefore, no statement can be made about the fossil content. This often complicates the stratigraphic classification of dolomitic rock formations.

Dolomite is a rock that is found all over the world and is often naturally associated with limestone. In Europe, dolomites are very common in the geologically young Alps. Very thick deposits are found in the eastern and southern Alps (including the Dolomites) as well as in the Carpathians and Apennines.

Formation

Dolomite rocks were formed either through the primary precipitation of dolomite or through the secondary dolomitization of calcareous mud. Recent research in the lagoons in Brazil indicates the import roll of Sulphur bacteria and putrefaction in the genesis of dolomite. The corresponding equation is:

$$CaCO_3 + MgSO_4 + CH_4 \longrightarrow CaMg(CO_3)_2 + H_2O + H_2S$$

or simplified, whereby $MgCO_3$ combines with the existing lime mud to

$$MgSO_4 + CH_4 \longrightarrow MgCO_3 + H_2S + H_2O$$

CH_4 represents the organic substance. The magnesium comes from concentrated seawater. Under calm water conditions and with high evaporation rates, as can prevail in the lagoons of tropical reefs, the salt content in the lagoon water increases and there is hardly any exchange between the oxygen-rich water in the upper part of the water column and the water in the pore space of the sediment. This favours the decomposition of the organic matter contained in the sediment through putrefaction and thus the dolomitization of the sediment. Reef rocks are relatively often dolomitized. This may be partly due to the porosity of the reef, which allows the solutions to circulate even at greater depths, and partly (at least in coral reefs) because the coral limestone consists of the unstable mineral aragonite, which makes the transformation easier.

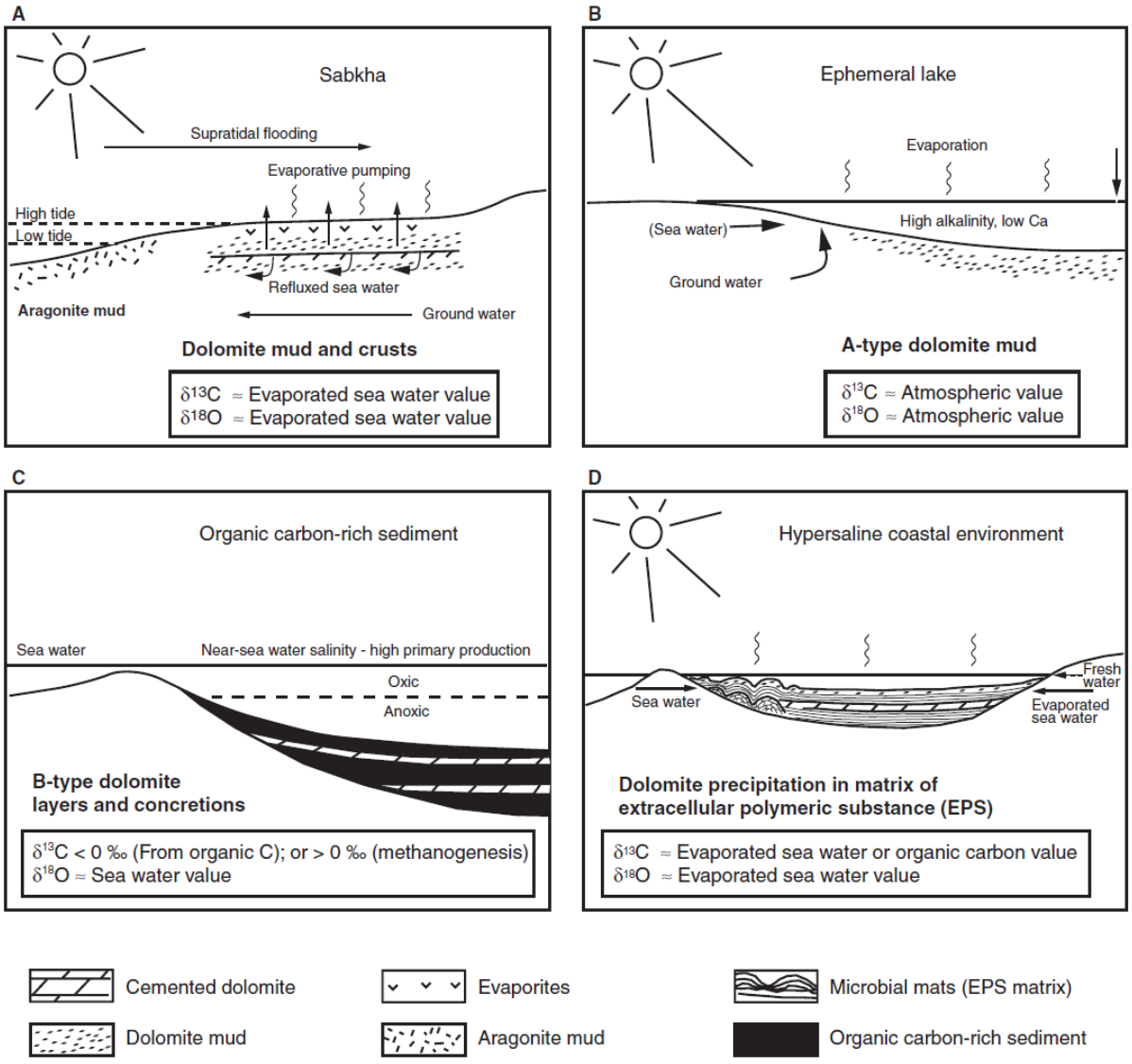

Schematic summary of different models of dolomite formation developed for modern environments: (A) sabkha model; (B) hypersaline/restricted lagoon (Coorong model); (C) organogenic dolomite model; and (D) microbial dolomite model. *[Source: P. H. Meister, P. Brack, S. Bernasconi, 2013: Dolomite formation in the shallow seas of the Alpine Triassic, Article in Sedimentology · Feb. 2013, DOI: 10.1111/sed.12001]*

Foraminifera

Foraminifera are separated into the planktonic and the benthic foraminifera on the basis of their life strategy. Planktonic foraminifera are represented by many species with worldwide occurrence in broad latitudinal and temperature belts, floating in the surface or near-surface waters of the open ocean as part of the marine zooplankton. Benthic foraminifera are as successful as the planktonic foraminifera group and even more abundant in modern seas and can live attached or free, at all depths.

Foraminifera typically produce a test, or shell, which can have either one or multiple chambers, some becoming quite elaborate in structure. These shells are commonly made of calcium carbonate (CaCO3) or agglutinated sediment particles. Over 50,000 species are recognized, both living (6,700–10,000) and fossil (40,000). They are usually less than 1 mm in size, but some are much larger, the largest species reaching up to 20 cm.

The most striking aspect of most foraminifera are their hard shells, or tests. These may consist of one of multiple chambers, and may be composed of protein, sediment particles, calcite, aragonite, or (in one case) silica. Some foraminifera lack tests entirely. Unlike other shell-secreting organisms, such as molluscs or corals, the tests of foraminifera are located inside the cell membrane, within the protoplasm. The organelles of the cell are located within the compartment(s) of the test, and the hole(s) of the test allow the transfer of material from the pseudopodia to the internal cell and back.

Benthic foraminifera

Benthic foraminifera live at all depths of the ocean, or in brackish/freshwater habitats, as either free-floating or attached organisms. Benthic foraminifera include two major types of foraminifera. The small benthic foraminifera, which have simple internal structures, and the larger benthic foraminifera, which have complicated internal structures and occur abundantly in the shelf regions of most tropical and subtropical shallow marine, carbonate-rich environments (Boudagher-Fadel and Price, 2013). The larger benthic foraminifera are not necessarily morphologically bigger than small benthic foraminifera, although many are, but they are uniquely characterized by having internally complicated tests. While one can identify small benthic foraminifera from their external morphology, one must study thin sections to identify larger benthic foraminifera from their internal test architecture. Larger benthic foraminifera develop complicated endoskeletons, which are reproduced precisely with each successive generation. These internal structures permit the taxa of such microfossils to be accurately identified, even when they are randomly thin-sectioned.

Large benthic foraminifera

All larger benthic foraminifera (LBF) are marine and neritic and live in oligotrophic reef and carbonate shoal environments (BouDagher-Fadel, 2008). Living forams occupy low-latitude areas and are most prolific in nutrient-deficient, warm, shallow seas. They are key in the production of carbonate sediment and are most often associated with coralgal reefs (BouDagher-Fadel, 2008).
The fossil record indicates that a similar distribution of foraminifera seen today was prevalent during the Mesozoic and Cenozoic. Sea temperatures over the last 65 million years can be approximated by living foraminifera (McMillan, 2000). In living forams, the minimum temperature tolerated is 18 degrees (Celcius) and the maximum water depth tolerated is 35 meters (Murray, 1973; BouDagher-Fadel, 2008). As a rule, the presence of larger benthic forams in the fossil record indicates a warm environment and the absence of them indicates a cooler environment.

Water depth, as a secondary factor, is another parameter that affects indirectly the distribution of larger benthic foraminifera (BouDagher-Fadel, 2008). Light intensity, temperature and hydrodynmaic energy decrease with depth. Some larger foraminifera (amphistegina) become flatter, with thinner outer walls, with increasing water depth and decreasing light. Imperforate foraminifera (miliolines) are restricted to shallower depths than perforate forms, however, both forms house symbionts and the dependence on light for their symbionts limits their distribution to the photic zone.

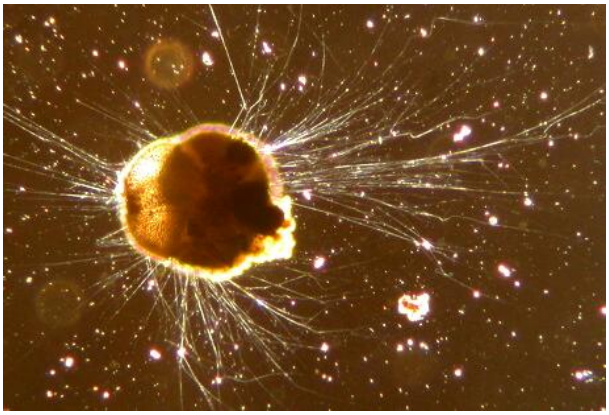	*Live Ammonia tepida (Rotaliida) benthic foraminiferan collected from San Francisco Bay. Phase-contrast photomicrograph by Scott Fay, UC Berkeley, 2005* *https://www.wikiwand.com/de/articles/Foraminiferen* *(https://creativecommons.org/licenses/by/2.5/deed.en)*
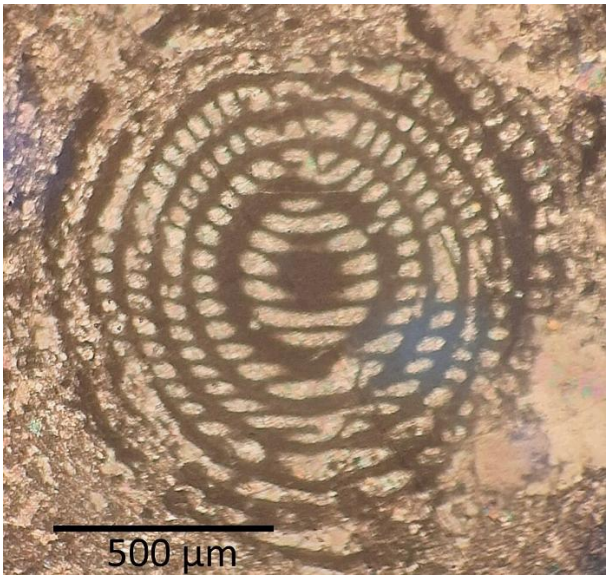	Alveolinidae Alveolinidae is a family of spheroidal to fusiform milioline foraminifera with multiple apertures and complex interiors in which chambers are subdivided into chamberlets and subfloors interconnected by passageways. In living individuals the pseudopodia emerge through the multiple apertures test. Alveolinids first appeared near the beginning of the Late Cretaceous, about 100 million years ago, some 150 million years after the superficially similar fusulinids became extinct at the end of the Permian. https://www.wikiwand.com/en/search?q=Alveolinidae, ViriatoLusitano *https://creativecommons.org/licenses/by-sa/4.0/deed.en*

Nummuliten

Die Familie tritt in der obersten Kreide fossil in Erscheinung und erlebte ihre Blütezeit im frühen Tertiär, hier vor allem in der Tethys. Im Paläogen (Alttertiär) war die Gruppe besonders artenreich vertreten und bildete die sogenannten Nummulitenkalke aus. Die Gattungen Assilina (†) und Nummulites sind Leitfossilien des Tertiärs.[1]

Die kalkigen Schalen der Nummuliten konnten sich nach deren Tod in erdgeschichtlicher Vergangenheit zu so großen Massen anhäufen, dass sie gesteinsbildend wurden, so beispielsweise bei den Nummulitenkalken aus dem Alttertiär.

Heterogestina (Familie Nummulitidae,

Neogene, Agio Fotia NE Crete

Dasycladaceae, Family of algae

https://www.wikiwand.com/en/articles/Dasycladaceae

Dasycladaceae

The Dasycladaceae is one of the two extant families of green algae of the order Dasycladales. When found in Palaeozoic limestones, they typically indicate depositional depth of less than 5m. In biology, an extant group is one which has survived to the present day, and so it is a living group. This distinguishes it from an extinct group.

Milankovitch cycles

Milankovitch cycles describe the collective effects of changes in the Earth's movements on its climate over thousands of years. The term is named for Serbian geophysicist and astronomer Milutin Milanković. In the 1920s, he hypothesized that variations in eccentricity, axial tilt, and precession resulted in cyclical variation in the solar radiation reaching the Earth, and that this orbital forcing strongly influenced the Earth's climatic patterns.

Similar astronomical hypotheses had been advanced in the 19th century by Joseph Adhemar, James Croll and others, but verification was difficult because there was no reliably dated evidence, and because it was unclear which periods were important.

Now, materials on Earth that have been unchanged for millennia (obtained via ice, rock, and deep ocean cores) are being studied to indicate the history of Earth's climate. Though they are consistent with the Milankovitch hypothesis, there are still several observations that the hypothesis does not explain. *[Milankovitch cycles - Wikipedia]*